POLITECNICO DI TORINO

Master Degree Course in Biomedical Engineering

Master Degree Thesis

Characterization of specific body segments at high and low frequencies using a bioimpedance fitting method in the context of the SINTEC Project

Supervisor:
Prof. Monica Visintin
Co-supervisor:
Prof. Guido Pagana

Candidate:
Rocco Calzone

Academic Year 2018-2019

Acknowledgements

I would first like to thank my supervisor Prof. Monica Visintin for her valuable suggestions during the thesis writing period and my co-supervisor Prof. Guido Pagana for his medical recommendations and for giving me the possibility to have my first study abroad experience.
I wish to express my sincere gratitude to Prof. Robin Augustine for welcoming me with open arms at Uppsala University in Sweden and Dr. Mauricio David Perez for his hard work and precious help. This thesis would not have been realized without their support, dedication and participation. I would also like to thank the members of the Microwaves in Medical Engineering Group (MMG) for providing a pleasurable working atmosphere. Thank you Javad, Laya, Eric, Marwa, Viktor, Syaiful, Ida, Bappa, Pramod and Jacob.
I would also like to thank amazing people as Davide, Federica, Giulia, and Valentina for making my life easier in Sweden. How to forget my extraordinary French friends Yann and Magali who have accompanied me with good dinners and beers. A big thank you also to Alvin, Decio, Rafael, Jonas and Dimitris for being such good friends.
I am deeply grateful to my old friends Giuseppe Marasco, Giuseppe Cicala, Domenico, Tonio, Marco, Vincenzo, Antonio and Salvatore for supporting me throughout these years.
I am truly thankful to Emanuela for sharing most of time during my Master's degree studies and for her precious help. I wish also to thank Valerio with which I shared exams fever and good time at the same time, and Luca for his presence and valuable suggestions.
A big thank you also to my colleagues Max, Stefano, Rosy, and the Sardinian colony: Michele, Pippo, Nicolo, Daniele, Gianni, Fabian and Edoardo.
Last, but not least, I would like to say special thanks to my family. First of all, my parents Mario and Caterina for always making me shine. It's thanks to them that I'm here now.
I should also like to thank my brother, the one who taught me to grow up in the moment of need, in the difficult situations.
A big thank you also to my grandfather, like a second father to me, who taught me the real values in life. I can never learn enough from him.
I would also like to thank Olga, for always having a way of making me feel better. My cousins, aunties and uncles deserve my heartfelt thanks as well.

Summary

Wearable body sensors are rapidly becoming part of people's everyday life. The use of such devices is important for constantly monitoring vital signs; for this reason, they are taking place not only in the biomedical scenario but also in sport performances and in the context of well-being. In this thesis, a bioimpedance-based algorithm for the characterization of the human body tissues is proposed to help to optimize sensors and antenna design in the context of the SINTEC Project. The H2020 European project SINTEC is intended to create communication platforms where two main innovations are integrated: soft epidermal electronics and intra-body communication based on fat tissue as a transmission channel. The novel platform will be included in a system that consists of a master node for the data collection of physiological parameters (heart rate, body temperature, blood pressure, respiratory rate, etc.) from different sensor nodes located in specific areas of the body. To ensure the proper functioning of the innovative technique based on the intra-body communication, it is necessary to design an adequate implantable antenna that radiates radio waves inside the body. Thus, the main purpose of this thesis is to understand the conduction phenomenon, the impedance parameters and other physical properties in biological materials. In particular, specific body segments such as chest, upper arm, forearm and leg have been analysed and considered as strategic parts where the future SINTEC sensor patch can be comfortably connected to. Significant localized biological components such as total body water, intra and extracellular water, fat mass, and fat-free mass (which includes all the human body tissues except the fat tissue) have been investigated by using bioimpedance methods which are low-cost, easy to use and non-invasive as they do not use ionizing radiation, as well as they do not interfere with devices such as defibrillators or pacemakers. The experiment was performed by using disposable adhesive patches and a microwave sensor, which have been properly applied on ten volunteers to evaluate the body tissues at both low and high frequencies. Due to the widespread use and good estimation performance, an impedance plane fitting method based on the Cole-Cole plot was implemented. This is done to estimate two important parameters that play a fundamental role for the estimation of the aforementioned biological components. In addition to the bioelectrical impedance data collection, the output data of a microwave

sensor were utilized in combination with a study on tissue compressibility to get an in-depth study useful to understand what type of tissue is being analysed. Furthermore, to compare the achieved results, reference values found in the literature have been used even though some characteristic values are not present because of the different location of the electrodes which cover different areas of interest. Nevertheless, reasonable values have been obtained with respect to the reference values: mean absolute errors of 3.70 kg for fat mass and 4.38 kg for fat-free mass have been found considering participants whose anthropometric characteristics are very similar to the ones found in the literature; mean absolute errors of 3.98 kg and 3.24 kg for extracellular and intracellular water associated with subjects' chest respectively; mean absolute errors of 0.79 kg for extracellular water of leg and 1.47 kg for intracellular water of leg have been found. Moreover, since this study was conducted not only to analyse convenient body segments in which the SINTEC sensor patch can be applied but also to guarantee the intra-body communication, in this thesis the upper arm was chosen to be considered as a key position where this type of communication could be guaranteed. Finally, a clustering method is presented for the validation of the obtained results where three clusters have been picked for its implementation by making a consideration on the subjects' weight. Future developments and suggestions on how to improve the present research study are also given in the last chapter. An important step before applying the final SINTEC sensor patch to human subjects will be its application on phantom-based demonstrators, which will mimic humans as much as possible.

List of abbreviations

BIA	Bioelectrical Impedance Analysis
BIS	Bioelectrical Impedance Spectroscopy
BMI	Body Mass Index
CT	Computed Tomography
DXA	Dual X-Ray Absorptiometry
ECG	Electrocardiography
ECF	Extracellular fluid
ECW	Extracellular water
FAT-IBC	Fat channel intra-body communication
FM	Fat mass
FFM	Fat-free mass
HR	Heart rate
IBC	Intra-body communication
ICF	Intracellular fluid
ICW	Intracellular water
MF-BIA	Multi-frequency bioelectrical impedance analysis
MMG	Microwaves in Medical Engineering Group
MRI	Magnetic Resonance Imaging
PM	Plasma membrane

PPG	Photoplethysmography
RR	Respiratory rate
SF-BIA	Single-frequency bioelectrical impedance analysis
SINTEC	Soft Intelligence Epidermal Communication Platform
SpO2	Oxygen saturation
SRR	Split Ring Resonator
TBW	Total Body Water
UU	Uppsala University
VNA	Vector Network Analyzer

Contents

Acknowledgements **1**

Summary **3**

1 Introduction **9**
1.1 Modern monitoring systems 10
1.2 Description of the SINTEC project 11
1.3 Motivation 13
1.4 Goal 14
1.5 Structure of thesis report 14

2 Background **15**
2.1 Electrical properties of body tissues 15
2.2 Fundamentals of bioimpedance and body components 19
2.3 Bioimpedance-based techniques 21
2.3.1 Introduction to BIA 21
2.3.2 Single-Frequency Bioimpedance Analysis 23
2.3.3 Multi-Frequency Bioimpedance Analysis 23
2.3.4 Bioelectrical Impedance Spectroscopy 24
2.3.5 Whole Body Bioimpedance Measurement 25
2.3.6 Body Segment Bioimpedance Measurement 27
2.4 Existing BIA devices 27

3 Materials and Methods **29**
3.1 Study participants 29
3.2 Study protocol 30
3.3 Performed experiment 31
3.3.1 Localized electrical impedance measurements 32
3.3.2 Two-electrodes versus four-electrodes method 34
3.3.3 Cole-impedance model 35
3.3.4 Body tissue characterization 40

3.4 Split Ring Resonator (SRR) 43
3.5 Compressibility test 47

4 Results and Discussion **49**
4.1 Bioimpedance moduli 50
4.2 Characteristic resistance values 53
4.3 TBW, ECW, ICW volumes 57
4.4 FFM and FM results 61
4.5 Compressibility and Resonance Parameters 63
4.6 Clustering algorithm 67

5 Conclusions and Future work **70**

Appendix A **73**

Appendix B **75**

Bibliography **77**

Chapter 1

Introduction

Human health state is defined by a variety of physiological parameters that must be constantly monitored as much as possible because they give information about the general individual's health. Due to that, most people are starting to be warned about this relevant issue in order to prevent any condition that impairs the normal functioning of the body. As a response to the consistent increase in the number of people suffering from various diseases, the medical research is always looking for:

- better diagnostic tools;
- accurate prognosis devices;
- expedited information transfer technologies;
- efficient patient management systems;
- other alternative medicine strategies.

It is evident that people are increasingly in need of accurate health monitoring systems that could be used both by physicians and patients to monitor physiological data relating to the history of a disease, its current status and its evolution over time. Furthermore, the development of new methods and devices is also appropriate to assess the body's reaction during sports and fitness activities, while watching television and in nocturnal monitoring for the evaluation of sleep quality. Overall, measuring vital signs such as body temperature, heart rate (HR), respiratory rate (RR) and blood pressure is important to improve people's needs belonging to three significant contexts: medicine, sport and wellness (Figure 1.1).

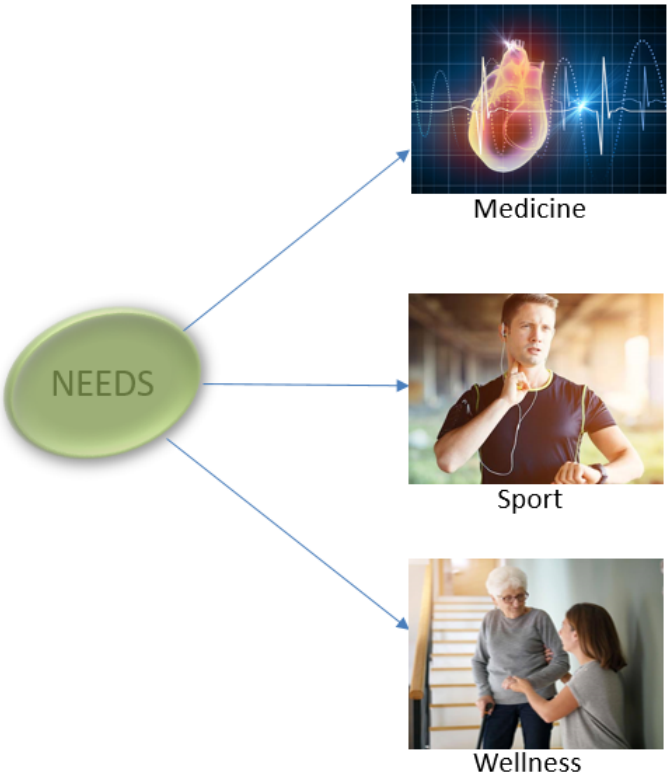

Figure 1.1: Wearable Body Sensors for improving people's quality of life

1.1 Modern monitoring systems

Over the years, modern monitoring systems have been renewed by replacing the complex and occasionally obsolete instrumentation with integrated systems; in fact, the development in the electronics sector has made available various sensors for checking vital signs. Pulse oximeters, heart rate and blood pressure monitors, thermometers, etc. are commonly used devices in hospitals and health specialized facilities. Physicians and medical experts use these devices to get a quick idea about the subject's heart rate, oxygen saturation (SpO2), body temperature and blood pressure.

Electrical and optical principles, most of which are based on the Tompkins algorithm [1], have been implemented in modern heart rate monitors to record heart signals. Electrical measurement techniques are normally implemented in medical devices and are based on electrocardiography (ECG) sensors for measuring the potential generated by different real-time dimensions of the heart caused by its contraction and expansion. Optical methods are instead implemented in modern smart bands, smartwatches (Figure 1.2), cell phones, etc. and they use photoplethysmography (PPG) sensors including light-based

technologies for measuring the blood volume due to the heart's pumping action.

Figure 1.2: Smartwatch developed by Apple Inc. capable of measuring the heart rate and other parameters

For the respiratory rate, which consists of counting the number of breaths made by an individual within a minute, different methods such as impedance pneumography, capnography and even the classic electrocardiogram have been used.

Modern health monitoring systems can also measure the human body temperature, which generally should be maintained within a range from 36.5 to 37.5 °C, by using different temperature sensors, and blood pressure, which basically represents an important indicator to predict health problems in the future.

Famous multinational companies such as Apple and Samsung are developing more and more smartwatches and bracelets allowing sport-loving people to track their cycle and control how many calories are being burned during outdoor activities. Moreover, utilizing monitoring systems can also be useful for elderly people to detect abnormalities in their body's physiological condition and rapidly go to a specialized facility to have adequate treatment.

1.2 Description of the SINTEC project

The aim of many companies and universities working both in the biomedical and electronic fields is to develop emerging, accurate, manageable, non-invasive technologies for monitoring physiological parameters that could be used anywhere, anytime. In this context, the SINTEC Project [2] proposes innovative stretchable systems that will enable expedited information transfer technologies in medical field as well as in sport performances. What the eight European partners from the Netherlands, Sweden, Italy, and

Spain involved in the aforementioned project will provide is the material science and how to use liquid metals to connect rigid components in soft, adhesive and extensible patches (Figure 1.3) that can be used several times and for longer periods.

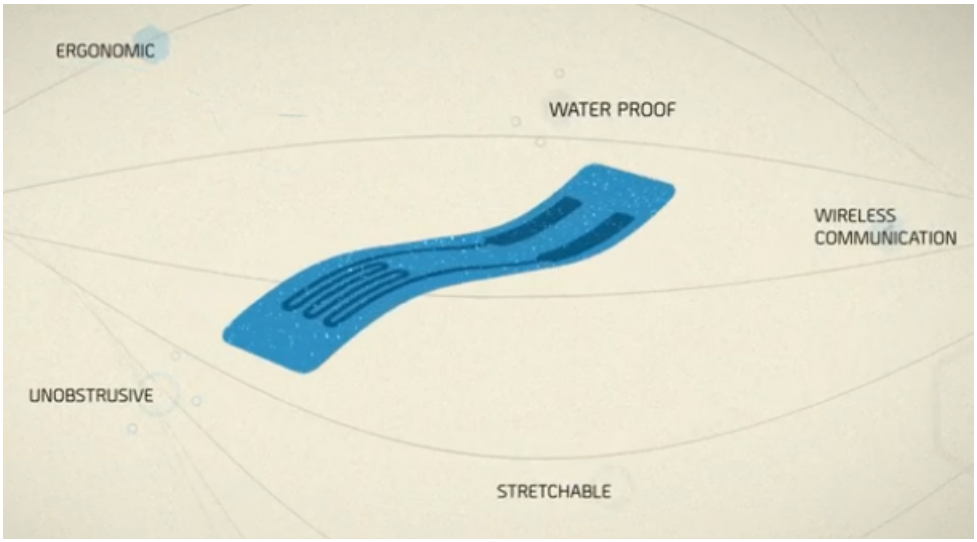

Figure 1.3: SINTEC's novel technology with an electronic card incorporated in a sweat resistant layer [3]

With a dynamic compliance and water repellent permeable encapsulation, the sensor patch will withstand vigorous action, sweating and water, making it ideal for an active life. Although an innovative stretchable RF-electronics including antenna, battery and several sensors in an electronic system will be used, the main modernization will be using the intra-body communication (IBC) [4] that uses fat tissue in the human body as a channel for data transmission in the microwave frequency range [5]. Furthermore, taking advantage of the human body as a conductive system, the novel fat channel intra-body communication (Fat-IBC) will be useful to avoid the dispersion of the signal allowing data transmission from many sensor nodes on the body (Figure 1.4). In addition, the privacy of the data transmitted will be guaranteed using the Fat-IBC.

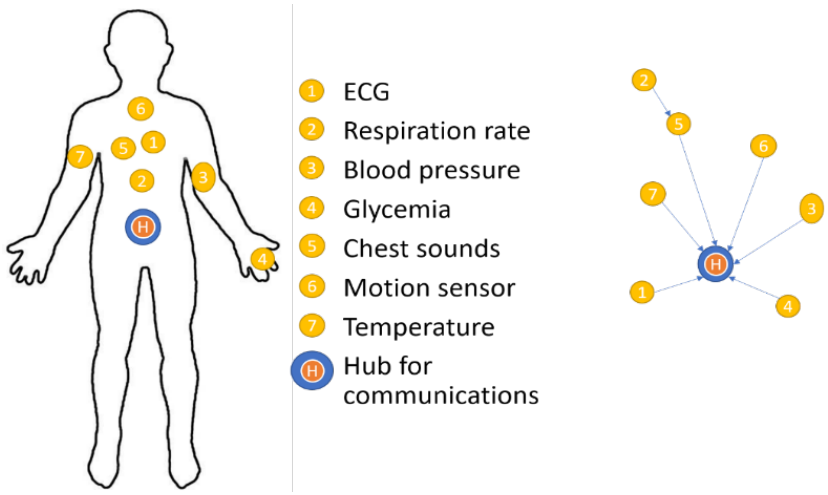

Figure 1.4: SINTEC's final architecture system [6]

The SINTEC's idea is to provide not only physiological data mentioned in Section 1.1 but also other important parameters such as:

- glycemia, i.e. the amount of glucose in the blood;
- body movements, while people practice sport or simply walking;
- chest sounds, which are related to the respiratory rate to diagnose any abnormal lung sounds.

As shown in Figure 1.4, the final system will have a master node that will receive all the information from different sensor nodes (located in different parts of the body) and will transfer the data to external devices via wireless technology. The data acquisition from specific body areas will be an interesting strategy to perform an adequate measurement of physiological parameters.

1.3 Motivation

In recent years, as many conventional techniques are awkward and inconvenient due to the restriction of subject's movement by cables, the need to develop new methods as comfortable as possible for human subjects is growing. Moreover, ensuring the reliability of the measurements is a crucial point and this can be improved by connecting the device directly to the skin. As discussed previously, many devices such as bracelets, patches, and bands are already available on the market but the SINTEC's novel technology will be more useful and convenient making the subject's life easier. Several solutions are being

studied to have devices capable of measuring vital signs in a very accurate and precise way; to overcome this, a proper characterization of the human body composition has been done. This work was made not only for the assessment of the body composition itself, but it will also be an essential part of the design of sensors and antenna that will be embedded into the future SINTEC sensor patch.

1.4 Goal

The main goal of the thesis is to better understand the distribution and properties of body tissues in humans to optimize sensors and antenna design in SINTEC. In particular, the proposed methodology is presented to try to tide over an important aspect concerning the antenna design which is one of the main components since it provides communication of the implant with external devices. Many researchers are trying to overcome this big challenge where a compromise between size, biocompatibility (i.e. the property of a material capable of being compatible with living tissue) and low-power consumption should be found to achieve a proper implantable antenna.

1.5 Structure of thesis report

The thesis work is summarily organized as follows:

- summary;
- five chapters;
- references.

Chapter 1 includes the introduction part of this study, current health monitoring systems and a brief overview of the SINTEC Project. Chapter 2 contains information about conventional methods used for the assessment of the human body composition. One of the techniques described in Chapter 2 has been chosen and successively analysed in Chapter 3, including the materials and methods that have been used. Chapter 4 shows results and measurements validation. Finally, Chapter 5 gives recommendations and future works on how to improve the present study.

Chapter 2

Background

The evaluation of body composition is important in the monitoring, management and diagnosis of numerous health outcomes (e.g. fat distribution and obesity) [7, 8], general health [9], muscle atrophy [10, 11], nutritional status [12], and fitness training assessment [12]. In this context, assessment of body composition is significant in clinical practice as in sports performance [13, 14]. Various techniques of assessing body composition such as computed tomography (CT) [15], dual energy X-ray absorptiometry [16], magnetic resonance imaging (MRI) [17] and anthropometric characterization [18] have been investigated although they are not accurate, extremely expensive and time-consuming [19, 15, 17, 20, 21]. On the other hand, bioimpedance-based methods for measuring body composition are low-cost, non-invasive and easy to use [22]. To understand how bioimpedance techniques work, firstly, a working knowledge about electrical properties of tissues, the meaning of bioimpedance itself and the definition of body compartments for determining the body composition is described; secondly, a detailed description of the bioimpedance-based techniques is presented. The final method used to measure body composition will play a relevant role in order to optimize sensors and antenna design in the SINTEC project.

2.1 Electrical properties of body tissues

As an electric current flows into a metallic conductor because of the presence of free electrons, electrical conduction in biological tissues develops due to the movement of mobile ions within the human body [23]. Therefore, biological tissues are characterized by electrical properties that depend on all the external fluid that surrounds the cells, called extracellular fluid (ECF), the fluid located within the cell membrane, called intracellular fluid (ICF), and also the plasma membrane (PM) itself. ECF and ICF are made of ions, and sodium, potassium and calcium are the most important cations that contribute to the generation of ionic currents (Table 2.1) [24, 25]. The PM is instead formed by proteins and a phospholipid bilayer.

Important cellular ionic concentrations		
	INTRACELLULAR	EXTRACELLULAR
Na^+	10 - 20 mM	150 mM
K^+	100 mM	5 mM
Ca^{2+}	10^{-4} mM	1 mM

Table 2.1: Approximate concentration of ions in living tissue expressed in millimolar (mM)

Unlike ECF and ICF that act as conductors due to the presence of ions, the cell membrane behaves instead as a dielectric (i.e. any material capable of storing capacitive energy) because of the insulating nature of the lipids. However, the ions exchange from the external part to the internal part of the cell is allowed by the integral proteins, which form the transmembrane channels. To summarize, the ECF-PM-ICF structure (Figure 2.1) can be schematized as a capacitor, i.e. as a conductive-dielectric-conductive structure.

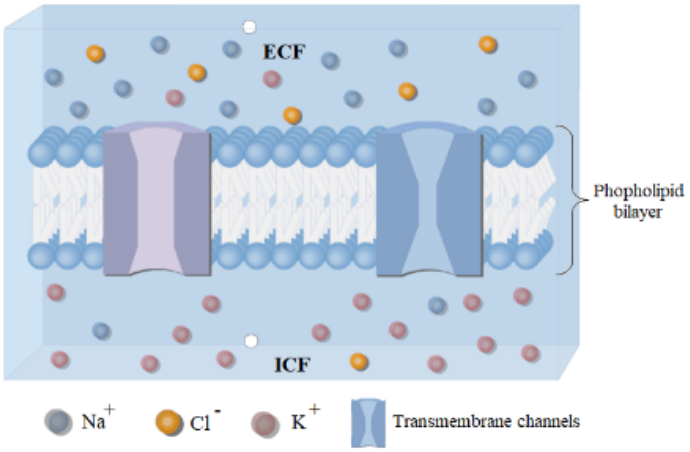

Figure 2.1: ECF-PM-ICF structure

For a better understanding of the conductive properties of biological tissues, the equivalent electrical circuit of tissue is shown in Figure 2.2.

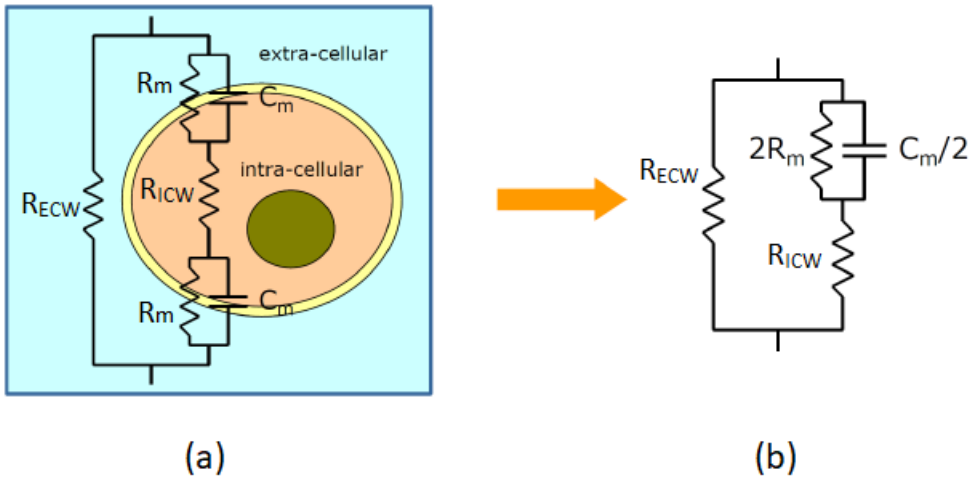

Figure 2.2: Electrical model of tissue

By injecting a current into the extracellular medium, electrical components of the circuit in Figure 2.2 can be determined: R_{ECW} is the resistance due to the current flow around the cell through the ECF; C_m is the capacitance that represents the current flow through the cell across the cell membrane; R_m is the resistance due to the current flow across the transmembrane ionic channel. When the current reaches the inside of the cell, it circulates through the ICF, flowing through the resistor R_{ICW}. Subsequently, the current leaves the cell flowing across the cell membrane through the R_m and C_m components. Due to the low conductivity of the plasma membrane, the value of the resistor Rm is very high, therefore typically the effect of Rm is neglected. However, whether a cell membrane acts as a capacitor or resistor is dependent upon the frequency of the current applied. At low frequencies, the current flows in the outer part of the cell because the cell membrane behaves as an insulator, therefore the current does not penetrate it. In contrast, when the frequency increases, the insulating effect of the plasma membrane decreases; in particular, if the frequency exceeds 50 kHz [26], the electric current is able to flow both in the ICF and ECF (Figure 2.3).

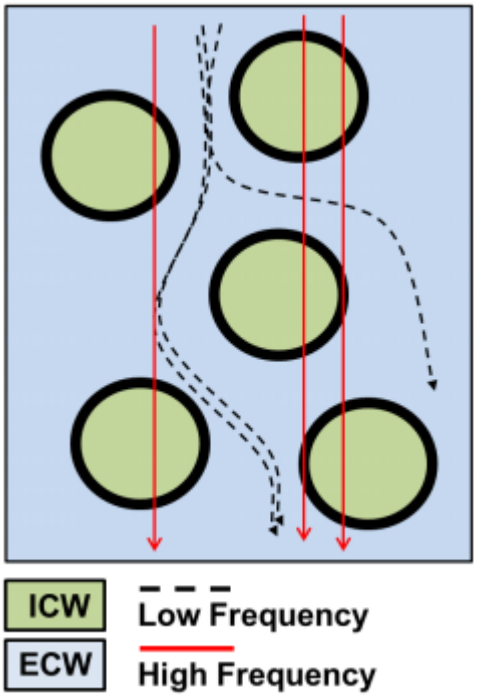

Figure 2.3: Current paths within the ECF and ICF [27]

As mentioned before, the movement of mobile ions in the biological medium will result in a current flow which depends on the conductivity of the specific tissue [25] that indicates how well the charges can move within the material. The complex electrical properties of tissue depend on bound charges, which include the electrical double layers and polar molecules (e.g. proteins). Moreover, the electrical behaviour of tissues is time-varying due to the presence of a displacement current. In the presence of an electric field, electrical charges can be polarized or shifted resulting in an important parameter called permittivity. This displacement of the electrical charges within different tissues will express different characteristic responses, resulting in a distribution of relative permittivities $\varepsilon^*(\omega)$ defined as:

$$\varepsilon^*(\omega) = \varepsilon_\infty + \frac{\varepsilon_S - \varepsilon_\infty}{1 + j\omega\tau} \tag{2.1}$$

where ε_∞ represents the high-frequency permittivity where polarization is minimal or almost zero, ε_S is the low-frequency permittivity where the displacement of the electrical charges is maximal, τ represents the characteristic relaxation time of the specific tissue and ω is the angular frequency. Nevertheless, relative permittivity and conductivity vary from tissue to tissue and are frequency-dependent parameters; due to that, three important

regions for evaluating the frequency dependence, denoted as dispersion, in biological tissues have been investigated [28]:

- α-dispersion → within this region, the dispersion is mostly caused by tissue interfaces, for example the cell membrane (frequency range: from 10 Hz to few kHz);
- β-dispersion → where the dispersion is related to organic macromolecules and the polarization of cell membranes (frequency range: from 1 kHz to several MHz);
- γ-dispersion → in this region, the dispersion is associated with the polarization of water molecules (frequency range: >10 GHz).

To conclude, studying the electrical properties of body tissues and the behaviour of the human body when it is subjected to electric field in different frequency ranges is important to comprehend the conductance phenomenon and the impedance parameters in biological materials which will be discussed in the next section.

2.2 Fundamentals of bioimpedance and body components

Bioimpedance (or biological impedance) is a measure of how well the body impedes electric current flow [29]. By injecting an electric current I into the body and measuring its voltage V, the bioimpedance Z can be estimated (Figure 2.4).

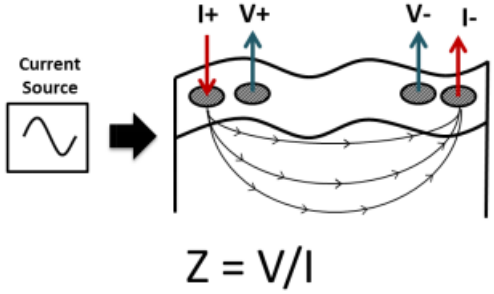

Figure 2.4: Bioimpedance measurement on the body

From an electrical point of view, the impedance Z is defined as a complex quantity that can be represented in the following ways:

- **the cartesian form** → in this case, the impedance is determined by the relation Z=R+jX_C, where R is the resistance (real part) and X_C is the reactance (imaginary part);

- **the polar form** → the impedance is defined by the relation Z = A·exp(jϕ), where A is the magnitude of the total impedance and ϕ represents the phase angle of the total impedance.

Basically, the resistance R of an object (e.g. a cylindrical-shape object for emulating a body segment) is defined considering its length l (cm), surface area S (cm^2) and resistivity ρ ($\Omega\cdot$ cm) as shown in equation 2.2:

$$R = \rho \cdot \frac{l}{S} \tag{2.2}$$

while the reactance X_C (Ω) is determined as shown in equation 2.3 and it is inversely proportional to the signal frequency f (Hz) and capacitance C (Farad):

$$X_C = \frac{1}{2\pi f C} \tag{2.3}$$

In body tissues, the resistance R depends on the amount of water in the specific body segment, whereas the reactance X_C is due to the capacitive effect of the plasma membrane [21]. By multiplying the numerator and the denominator by the length l of the object in eq. (2.2), the body volume V_B (see equation 2.4) can be determined:

$$V_B = S \cdot l = \rho \cdot \frac{l^2}{R} \tag{2.4}$$

where V_B represents the volume used for estimating the body composition and it is expressed in cubic centimetres (cm^3). Several factors can influence the impedance measurement; for example a body segment of larger diameter will obstruct the current to a lesser degree (since there is a greater volume to conduct the current), a short body segment results in a lower impedance than in a long one, and also, since there is an inverse relationship between impedance and temperature, a warm body segment will allow more electricity than a cold one. However, a relationship of how bioimpedance is linked to body volume composition using only the body segment length and impedance has been shown. With regard to the biological components, the body segment being measured can be broadly divided into fat-free mass (FFM) and fat mass (FM). The former includes all the human body tissues except the fat tissue, while the latter consists of the adipose tissue (or fat) which can be divided into two more categories: non-essential fat and essential fat [30]. By applying an electric current to the body, only a small amount of it will pass through the FM due to the poor quantity of water (about 20%), whereas a reasonable

amount of current will flow into body's vital tissue and cells that form the FFM. For this reason, FM is considered as an excellent resistor and it can be calculated as follows:

$$M_F = M_T - M_{FF} \tag{2.5}$$

where M_F is the fat-free mass (FFM) and M_T represents the subject's body weight (kg). In contrast, FFM is defined as the conductive volume that allows the injected current to flow more easily into the human body. Moreover, FFM is mostly made up of 73% of the total body water (see equation 2.6) in normal subjects:

$$M_W = 0.73 \cdot M_{FF} \tag{2.6}$$

where M_W is the total body water (TBW) expressed in kg and it contains both ECF and ICF. A higher TBW indicates more FFM, since effectively all of the TBW is located in the FFM. An explanation of the body compartments and essential parameters to determine the human body composition is done. In many bioimpedance measurement techniques, these indicators such as FM, FFM, TBW, etc. have been investigated and obtained considering the entire body or body segments separately.

2.3 Bioimpedance-based techniques

Due to the portability, efficiency and non-invasiveness of bioimpedance-based techniques, they offer many advantages in estimating the human body composition compared to other conventional methods. For example, bioimpedance techniques do not use ionizing radiation and do not interfere with devices such as defibrillators or pacemakers. Moreover, bioimpedance analysis techniques are easy to use (the presence of medical experts or radiologists is not required) and much less expensive than other methods such as dual X-ray absorptiometry (DXA) and magnetic resonance imaging (MRI) [19]. Finally, bioimpedance-based techniques are more accurate than body mass index (BMI), skinfold and anthropometric measurements [14] and provide reliable results with predicted errors between 3 - 8% for TBW, FFM, etc. [14]. As a result, bioimpedance-based techniques derived from the well-known Bioelectrical Impedance Analysis (BIA) technique are described in the following sections, as well as some of their limitations are elucidated in the present work.

2.3.1 Introduction to BIA

One of the most widely used bioimpedance analysis techniques is known as Bioelectrical Impedance Analysis (BIA) which is performed to estimate the body composition of the whole body [31] or segmentally [32] by using different operating frequency ranges. The

basic principle of BIA is that an electric current circulates into the body and the voltage is measured in order to estimate the biological impedance of the body (Figure 2.5). By applying a certain input current into the body, the output current will be lower depending on the amount and nature of tissue through which it passes.

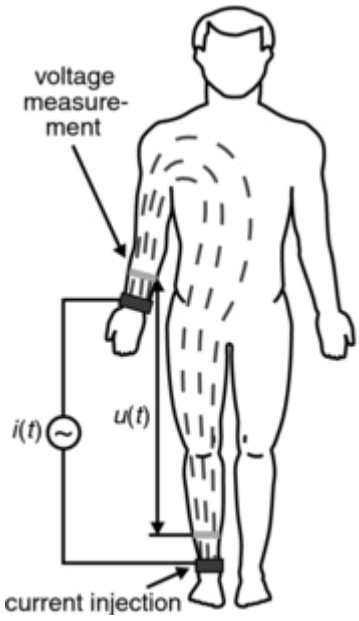

Figure 2.5: Principle of Bioelectrical Impedance Analysis [33]

Most BIA devices use a four-electrodes configuration, also known as tetrapolar configuration (Figure 2.6), in which two electrodes inject the current while the other two electrodes detect the voltage. There are a lot of tetrapolar devices; for example, a commercial device (similar to a bathroom scale) is comprised of four metal contact points where the subject has to stand on while the current is passed through his/her feet. Although it seems to be a suitable tool, the problem is that this device is not able to estimate the subject's upper body composition, but only the lower one because of the locations of the electrodes.

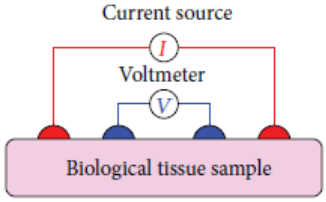

Figure 2.6: Tetrapolar configuration for the detection of bioimpedance

As mentioned in Section 2.2, the adipose tissue is only about 20% of water, therefore it is not a good conductor and it has a high impedance. On the other hand, body muscles have a relatively low impedance as they are made up of about 75% of water. Based on these differential effects of various tissues on the applied electrical current, BIA can be useful in determining different parameters such as FM, FFM, TBW, etc. To this end, several BIA techniques that use different areas of interest, operating frequency and working principle are explained.

2.3.2 Single-Frequency Bioimpedance Analysis

In the single-frequency bioelectrical impedance analysis (SF-BIA) an electric current of 500 microamperes (that is not dangerous for biological tissues) at a single frequency of 50 kHz or more is injected to measure the bioimpedance of the entire body [34]. In order to estimate the body compartments, SF-BIA utilizes empirical equations [21] which are based on a relationship (aforementioned in equation 2.4) that depends on the conducting length and bioimpedance, as well as factors such as race, age, sex and other anthropometric parameters. Furthermore, as measuring subjects' height is easier than their conducting length, the equation 2.4 can be modified as follows:

$$M_W = k \cdot \frac{H^2}{R} \tag{2.7}$$

where H is the body height (cm), R is the resistance of the body segment (Ω), and k ($\Omega\cdot$ cm) is a coefficient which matches the ideal cylinder to the real geometry. Although SF-BIA methods have been investigated to assess FFM, TBW and FM for normal hydrated subjects, this technique is not suitable for overhydrated or dehydrated subjects [35] who would provide inaccurate measurements.

2.3.3 Multi-Frequency Bioimpedance Analysis

The multi-frequency bioimpedance analysis (MF-BIA) is very similar to SF-BIA with the difference that in MF-BIA the bioimpedance measurements are typically performed from 5 kHz to 1 MHz. The operating frequency to be used in this technique is very discussed: as reported in [36] a frequency range from 100 Hz to 1 kHz has been used to estimate TBW and ECF; in [20] a bioimpedance analyser was set with a frequency range between 5 kHz and 1 MHz; other authors stated that low frequency is typically less than 20 kHz and high frequency is more than 50 kHz in [37]. Generally, the MF-BIA technique estimates ECF more accurately than SF-BIA technique; however, as reported in [38] the MF-BIA technique illustrates less sensitivity for the detection of fluid shifts between ICF and ECF.

2.3.4 Bioelectrical Impedance Spectroscopy

Bioelectrical impedance spectroscopy (BIS) works on the same principle that is used in MF-BIA, but in addition, further processing after the data collection is provided. In order to correctly estimate the parameters C_m, R_{ECW} and R_{ICW} of the model in Figure 2.2, the bioimpedance measurements have to be performed within a band from very low (e.g. 5 kHz) to very high (e.g. 1 MHz) frequencies [24,43]. Since the cell membrane acts as an insulator at very low frequencies, ideally the resistance at zero frequency (R_0) corresponds to the extracellular resistance (R_{ECW}). By the same token, at very high frequencies the plasma membrane behaves like a good conductor allowing current to pass through both ECF and ICF; consequently, the resistance at infinity frequency (R_∞) is determined as the parallel combination of R_{ICW} and R_{ECW} as shown in equation 2.8:

$$R_\infty = \frac{R_{ICW} \cdot R_{ECW}}{R_{ICW} + R_{ECW}} \tag{2.8}$$

In this manner, all the resistances (R) and negative reactances ($-X$) calculated for each frequency in the predetermined range can be displayed using the Cole-Cole plot (Figure 2.7) [39].

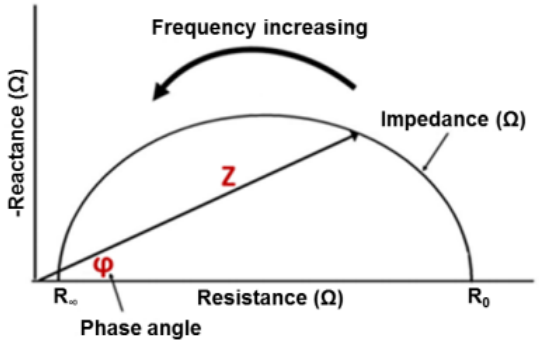

Figure 2.7: Cole-Cole plot for the characterization of R_0 and R_∞

The BIS technique is therefore based on extrapolating R_0 and R_∞ in order to estimate both ECF and TBW, respectively. One of the available BIS devices on the market is called Impedimed SFB7 that uses 256 frequencies from 3kHz to 1MHz to generate its Cole-Cole model [40]. An alternative method for assessing the body composition consists of utilizing empirical equations using the R_0 and R_∞ parameters obtained from the Cole-Cole plot. By replacing R_0 (which theoretically is equal to R_{ECW}) in equation 2.4, it is possible to

calculate the ECF volume (V_{ECF}) as:

$$V_{ECF} = \rho_{ECF} \cdot \frac{l^2}{R_{ECF}} \tag{2.9}$$

In the same way, ICF volume (V_{ICF}) can be estimated considering that R_∞ could be calculated through equation 2.8:

$$V_{ICF} = \rho_{ICF} \cdot \frac{l^2}{R_{ICF}} \tag{2.10}$$

Finally, TBW can be defined as the sum of ICF and ECF:

$$TBW = V_{ECF} + V_{ICF} \tag{2.11}$$

As stated in [41], different resistivities that vary between body segments and sexes are reported in Table 2.2.

	Women [$\Omega \cdot cm$]	Men [$\Omega \cdot cm$]
ρ_{ECF} Arm	64 ± 14	67 ± 8
ρ_{ECF} Trunk	172 ± 21	159 ± 24
ρ_{ECF} Leg	99 ± 15	98 ± 13
ρ_{ICF} Arm	191 ± 36	194 ± 29
ρ_{ICF} Trunk	266 ± 42	250 ± 38
ρ_{ICF} Leg	281 ± 45	281 ± 43

Table 2.2: Segmental resistivity for men and women

As the BIS method uses the resistances obtained at zero and infinite frequencies, it is said to be more accurate than other BIA methods which are based on empirical equations [20, 21, 42, 43].

2.3.5 Whole Body Bioimpedance Measurement

Whole body bioimpedance measurement (also known as whole body BIA) is the most commonly BIA procedure in clinical applications and it consists of attaching four electrodes to the foot, ankle, hand and wrist (Figure 2.8) so that the current can pass through the entire body [14, 16, 42].

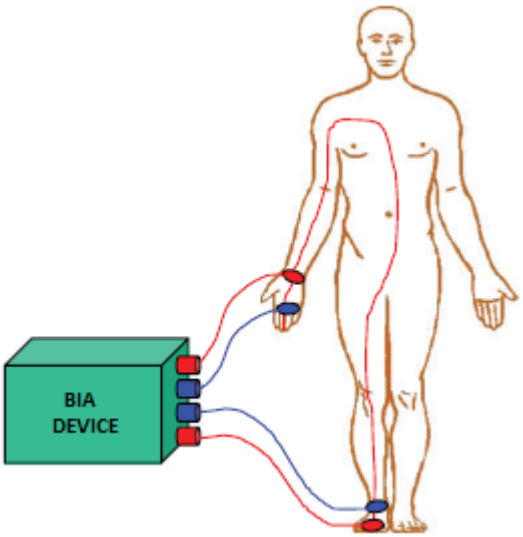

Figure 2.8: Whole Body Bioimpedance Measurement

Although this technique is the simplest one among the many BIA methods for estimating body composition, it provides clear estimation errors due to the hypothesis that the subject's length and cross-sectional area are considered as a uniform cylinder forming the body. Since the current flows across different types of tissues throughout the body, the conductivity is not constant and the cross-sectional area varies [21]. Consequently, changes in anthropometric and anatomical characteristics of the entire body and segments, in particular between subjects with similar statures, can provide large differences in estimated volumes [14, 21]. This limitation should not be problematic in healthy subjects, as the body fluids are typically at a stable level within the body and therefore, the resistance of any segment is representative of the entire body.

2.3.6 Body Segment Bioimpedance Measurement

In the body segment bioimpedance measurement (also known as segmental BIA) the impedance at specific body areas or segments can be estimated (Figure 2.9).

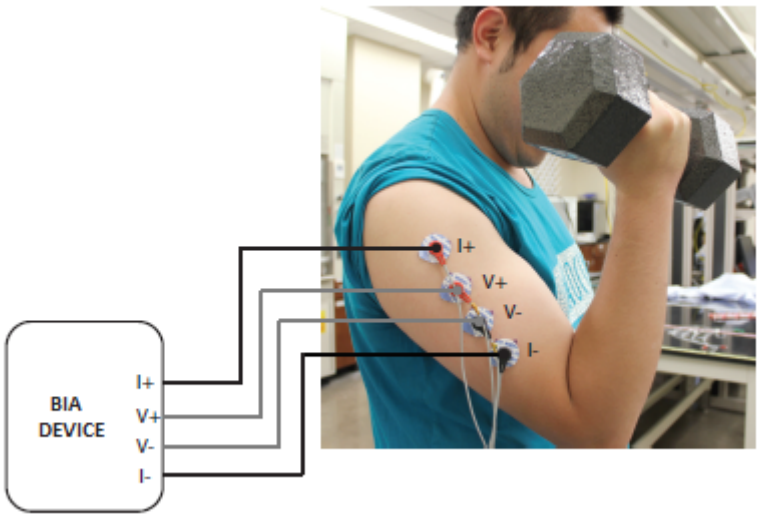

Figure 2.9: Bioimpedance measured from biceps tissue using tetrapolar configuration

Since the data collection is performed from the specific body district, segmental BIA is said to be the superior method of the BIA techniques used to assess the body composition [14]. In the clinical scenario, a comparison between whole body BIA and segmental BIA measurements is reported in [44] where patients for the treatment of peritoneal dialysis have been involved. Segmental BIA was shown to be very accurate in measuring ECF and ICF volume changes, whereas whole body BIA was revealed to be inappropriate in detecting these changes [44]. Furthermore, segmental BIA can be useful to understand specific fluids distribution of the body; for example, a medical expert may measure thoracic impedance to quantify fluid accumulating in a patient with congestive heart failure. In addition, in [21] relative errors up to 10-13% and 13-17% of FFM for legs and arms have been shown. However, segmental BIA is considered to be a valuable tool for assessing body composition in most studies [16, 19].

2.4 Existing BIA devices

There are a lot of BIA devices on the market with prices ranging from about $2,000 up to $24,000. Although such devices are very comfortable and easy to use, they do not estimate the body composition by using MF-BIA, BIS and/or segmental BIA. A list of

the commercial BIA devices is shown in Table 2.3.

Device	Electrode Style	Frequencies	Continuous Output	Portable	Output RAW Impedance	ECF/ICF Cabability	Cost (CAD)
BIA450 (Boidynamics Corp)	Whole body body	50 kHz	No	Yes	Yes	No	$2,200
Quantum V (RLJS Systems)	Five segment method	50 kHz	No	Yes	Yes	No	$4,350
MC-980Uplus (Tanita)	Five segment method	1,5,50,250 500,1000 kHz	No	No	Yes	Yes	$16,000
SFB7 (ImpediMed)	Single channel	4 kHz-1 MHz	Yes	Yes	Yes	Yes	$7,500
InBody 770 (InBody)	Five segment method	1,5,50,250 500,1000 kHz	No	No	Yes	Yes	$23,800
mBCA515 (Seca)	Five segment method	1 kHz-1 MHz	No	No	Yes	ECF only	$12,995
Multiscan 5000 (Bodystat)	Single channel	5 kHz-1 MHz	No	Yes	Yes	Yes	$17,495
BodyComp MF Hexa (SMT Medical)	Whole body	5,50,100,150 200,250 kHz	No	Yes	No	ECF only	$6,400

Table 2.3: Commercial BIA devices

The perfect BIA device should perform the bioimpedance measurements within a range of frequencies and from different parts of the body. The aforesaid Impedimed SFB7 is the most known typical system utilized for assessing the body composition, but it cannot estimate tissue composition continuously and even perform segmental analysis simultaneously [44]. Consequently, the BIA device can only be applied on a single body segment at a time resulting in difficulties in terms of tracking fluid displacements and very time-consuming multiple segments measurements. Commercial BIA devices are based on traditional gel electrodes which can be inappropriate for the estimation of body fluid volumes continuously because the conductive gel can dry during lengthy measurements, and a degradation of the signal quality can be revealed.

Chapter 3

Materials and Methods

Since the purpose of this study is to better understand the body composition in which the future sensor patch can be applied, specific human body segments are analysed. To this end, the choice of the bioimpedance-based method fell on the combination of segmental BIA and BIS. This was made because whole body BIA presents clear limitations in estimating body segment compartments, as discussed in Section 2.3.5. For this reason, segmental BIA was chosen to be used as it provides improved resolution over whole-body techniques and, once the data were collected, they were subsequently processed according to the BIS principles mentioned in Section 2.3.4.

In addition, a microwave sensor developed at Uppsala University and an evaluation of tissue compressibility are utilized to get an in-depth study regarding the overall characterization of tissue composition. Besides that, this chapter describes in detail the physical characteristics of the participants, the study protocol performed during the conducted experiment, and all the software and hardware components.

3.1 Study participants

The present study collected measurements from specific body areas of 10 subjects, including 7 males and 3 females, with an average age of 26.3 $\pm$ 11.5 years (where 11.5 is calculated as the arithmetic mean of the difference between the highest and lowest values), average weight of 65.52 $\pm$ 22.6 kg and average height of 170.5 $\pm$ 15 cm. More details can be found in Table 3.1.

Participant	Sex	Age	Weight [kg]	Height [cm]
1	Male	35	50.3	158
2	Male	24	62	174
3	Male	25	62.4	165.5
4	Male	39	95.5	178
5	Male	23	64.7	166.5
6	Male	24	70	172
7	Male	16	67.7	188
8	Female	24	70	172
9	Female	21	55	170
10	Female	32	57.7	161
AVERAGE	/	**26.30**	**65.52**	**170.50**
ST_DEV	/	**6.93**	**12.34**	**8.61**

Table 3.1: Characteristics of the participants

3.2 Study protocol

All participants were recruited from Uppsala University and informed written consent was obtained from each of them before their inclusion in the study (see Appendix A). During the protocol, each participant was seated, leaning against the back of a chair, and asked to relax his/her muscles. Each area of interest was cleaned with alcohol. Figure 3.1 shows the body segments from which the bioimpedance signals were picked up. Chest, upper arms, forearms and lower legs were considered essential parts where the SINTEC sensor patch will be comfortably connected to.

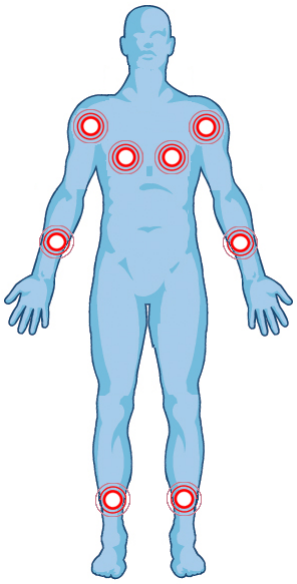

Figure 3.1: Bioimpedance measurements from specific body areas

An important observation was that acquiring data from the right side of the body or from the left side resulted in minimal differences, i.e. measuring the bioimpedance, for example, of the left forearm or right forearm from the same subject does not change much (this will be proved in Chapter 4). As a result, only the right side of the body was chosen to be analysed in order to make the procedure less time-consuming.

3.3 Performed experiment

The purpose of collecting these measurements is to provide details regarding the conduction phenomenon, the impedance parameters and other physical properties in biological materials. Human tissues are analysed both at high and low frequencies getting different output parameters. In the first place, localized impedance measurements have been collected and body compartments such as FFM, FM, ECW, ICW and TBW are estimated by using the R_0 and R_∞ parameters obtained from the Cole-Cole model. Secondly, for a better understanding of tissue composition under test, a split ring resonator (SRR) [45] is utilized, whose resonance is a function of the geometry and dielectric properties of the involved tissues. The output data of this sensor, which operates using non-ionizing microwave signals, are used in combination with a study on tissue compressibility and the acquired bioimpedance data.

3.3.1 Localized electrical impedance measurements

The localized bioimpedance measurements were performed using adhesive patches (Figure 3.2) developed by a Swedish company called Beneli [46]. To collect and store the impedance data from different parts of the body, only one commercial disposable patch per subject was used.

Figure 3.2: Beneli Patch Design: a) Bottom side; b) Top side.

The benefit of using the Beneli patch is that, instead of using a four-individual electrodes configuration which requires fixed electrode distances, the investigator cannot make any mistake in terms of distance. As it can be seen in Figure 3.2, the Beneli patch is based on tetrapolar electrode configuration and it is composed of:

- 4 carbon black connectors, two of which are used for current injection and other two for voltage measurement (see Section 3.3.2 for details).
- 4 silver/silver chloride (Ag/AgCl) traces, which represent the conductive part that occurs only over the third dimension (Z-axis). This guarantees that the electrical conductivity take place in one direction, therefore it consists of anisotropic material.
- 4 electrode sites, which are made of a combination of Ag/AgCl and hydrogel. The latter provides strong match to the skin-electrode interface.

The electrical impedance measurements were collected using a Keysight E4980A Precision LCR Meter [47] which has two connectors used for current injection and other two

for voltage measurement. The detailed measurement setup is shown in Figure 3.3 and all the measurements were collected from 10 kHz to 1 MHz at 72 logarithmically spaced frequencies. This frequency range was used because both ICF and ECF can be analysed, therefore characteristic parameters mentioned in Section 2.1 can be estimated.

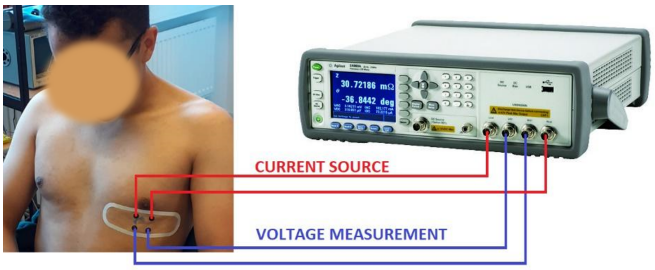

Figure 3.3: Measurement setup: the Beneli patch connected to the subject's chest and data collection using the LCR meter. The connection between patch and LCR meter was made by using four shielded crocodile clips (red and blue lines).

Before data collection, the LCR meter was calibrated using the open/short/load procedure as reported in [47] and it was connected to a computer for data acquisition using a LabVIEW application (see Appendix B). Examples of how the bioimpedance measurements were collected in other body segments are given in Figure 3.4.

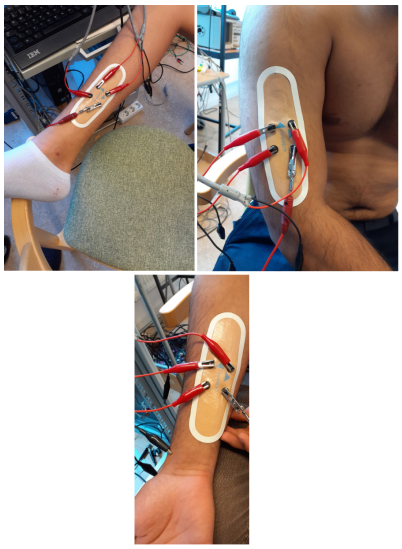

Figure 3.4: Bioimpedance measurements from different body segments: upper arm, forearm, lower leg

3.3.2 Two-electrodes versus four-electrodes method

Bioimpedance measurements can typically be performed in two ways: the two-terminal measurement technique and the tetrapolar measurement technique. In the former method the same two leads are both utilized to inject current into the body and to measure the potential difference, whereas in the latter method, two electrodes are used for current injection and other two for voltage measurement. Unlike the two-electrodes method, the tetrapolar technique removes series impedances and contact-resistance errors; thus, it is more used due to better accuracy in measuring low impedance, or at low frequencies [48]. However, the tetrapolar method setup is more complex to perform, as shown in Figure 3.5.

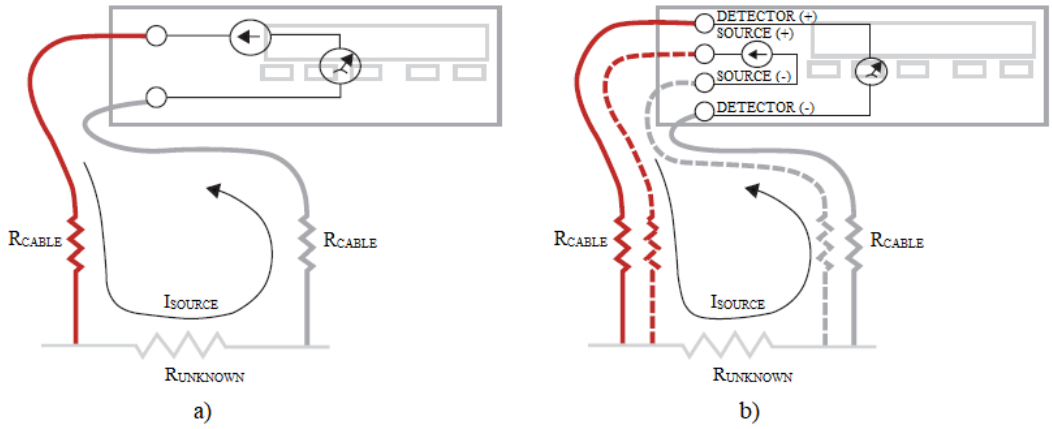

Figure 3.5: Measurement configurations: a) two-electrodes method; b) tetrapolar method

If only two cables are used, the current source travels along the same path used to measure the voltage drop (Figure 3.5 a). The test leads are not perfect conductors and have some intrinsic series resistances. By passing the current through the test leads, it is possible to detect not only the voltage drop across the unknown resistance, but also the voltage drop for each cable. In this way, the combined resistance of the positive cable, the negative cable and the unknown resistance is measured. Whenever the four test leads are used, the input electric current and the measurement can be separated (Figure 3.5 b). The terminals of the measuring instrument are called "Source" on the supply side and "Detector" on the voltage input side. The series resistances in the Source cables do not affect the current flow, while in the Detector cables the current flow is practically non-existent due to the high input impedance of the measuring instrument. This means that there is no voltage drop in the test leads. Therefore, only the voltage drop of the unknown resistor is measured due to the supply current flow passing through it.

3.3.3 Cole-impedance model

During the last decades, many studies have used the Cole-impedance model in biomedical applications including: changes in biceps tissue impedance collected during a fatiguing exercise protocol [49], estimation of the impedance of blood to monitor thrombus formation [50], development of a device for leg fluid volume measurements [44]. Nevertheless, fitting the bioimpedance data by using the Cole-impedance model is very common within segmental BIA and BIS techniques. In this way, a clear data visualization through the Cole plot and a significant data analysis through the Cole parameters can be obtained [51]. The Cole-Cole model is based on the following equation:

$$Z(\omega) = R_\infty + \frac{R_0 - R_\infty}{1 + (j\omega\tau)^\alpha} \tag{3.1}$$

where:

- $Z(\omega)$ is a complex function;
- R_∞ is the resistance at infinity frequency;
- R_0 is the resistance at zero frequency;
- ω is the angular frequency;
- τ is the inverse characteristic frequency.

Taking a look at the equation (3.1) and considering $j^\alpha = \cos(\alpha\pi/2) + j\sin(\alpha\pi/2)$, it is possible to decompose $Z(\omega)$ into resistance R and reactance X, in equations (3.2) and (3.3) respectively.

$$R(\omega) = R_\infty + \frac{(R_0 - R_\infty)(1 + (\omega\tau)^\alpha \cos(\alpha\pi/2))}{1 + 2(\omega\tau)^\alpha \cos(\alpha\pi/2) + (\omega\tau)^{2\alpha}} \tag{3.2}$$

$$X(\omega) = -j + \frac{(R_0 - R_\infty)(\omega\tau)^\alpha \sin(\alpha\pi/2)}{1 + 2(\omega\tau)^\alpha \cos(\alpha\pi/2) + (\omega\tau)^{2\alpha}} \tag{3.3}$$

Different fitting methods for electrical impedance data have been investigated to assess their adequacy to fit the Cole equation and estimate the Cole parameters [52]; some of them rely on a non-linear least squares fitting, other are based on the impedance plane fitting.

The non-linear least squares fitting methods consist of plotting the impedance in the following ways:

- Frequency versus real part of the impedance;
- Frequency versus imaginary part of the impedance;
- Frequency versus complex impedance.

The impedance plane fitting model technique instead is about plotting the resistance versus negative reactance as mentioned in Section 2.3.4. Due to the widespread use and best estimation performance [53], this method is used in this thesis to estimate the R_0 and R_∞ parameters from the collected bioimpedance data. Moreover, the impedance plane fitting methods have lower computational costs than the non-linear least squares fitting methods.

Non-linear least squares fitting methods

The purpose of the non-linear least squares fitting methods is to minimize the summed squared of the error between the data point and the fitted model:

$$min \sum_{i=1}^{N} e_i^2 = min \sum_{i=1}^{N} (y_i - \overline{y_i})^2 \tag{3.4}$$

where N is the number of data points included in the fit. These methods can be easily implemented in MATLAB®with the use of note functions such as fit, fmincon, lsqcurvefit, etc. [49, 44]. These functions provide the four Cole-Cole parameters R_0, R_∞, α and τ.

Impedance plane fitting method

The Cole-impedance model simulates a perfect semicircle, thus this method estimates its radius and complex centre. The points forming the semicircle are given by N bioimpedance values (see equation 3.5), which are associated to N frequencies (collected from 10 kHz to 1 MHz), acquired with one measurement from a specific body segment (Figure 3.6).

$$Z_n = X_n + jY_n \tag{3.5}$$

$$\text{n} = 1,\cdots,\text{N}$$

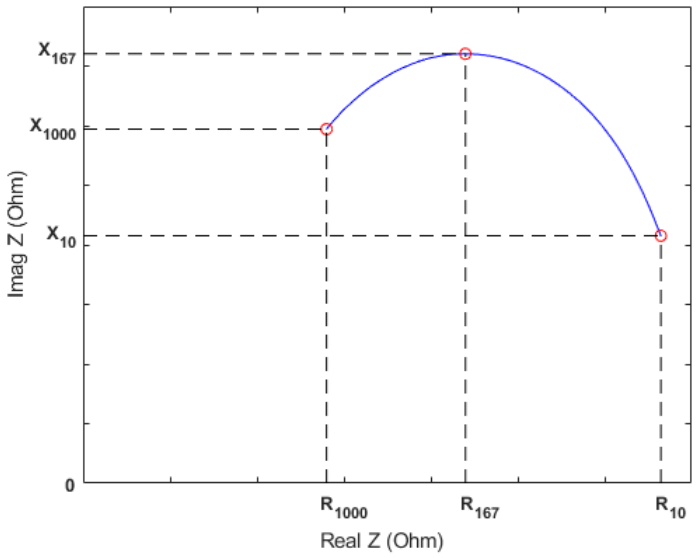

Figure 3.6: Example of N bioimpedance measurements estimated from subject's chest of participant 1 with resistances and reactances at specific frequencies

Figure 3.6 shows an example of N bioimpedance measurements (blue curve) plotted as resistances versus reactances, where R_{1000} - X_{1000}, R_{167} - X_{167}, and R_{10} - X_{10} are the resistances and reactances at 1MHz, 167 kHz and 10 kHz respectively. Given the centre C of the Cole semicircle and the impedance Z_n as:

$$C = x + jy \tag{3.6}$$

$$Z_n = X_n + jY_n \tag{3.7}$$

the distance R_n between C and Z_n can be defined:

$$R_n^2 = |C - Z_n^2| = (x - X_n^2) + (y - Y_n^2) \tag{3.8}$$

In order to get the best fitting of the curve, R_n has to be as small as possible, therefore the variance (equation 3.9) must be differentiated in the x and y component and subsequently these two components are set equal to zero.

$$Var\{R_n^2\} = \frac{1}{N}\sum_{n=1}^{N}\Big(R_n^2 - \frac{1}{N}\sum_{m=1}^{N} R_m^2\Big)^2 \tag{3.9}$$

The variance differentiation is given by the following equations system:

$$\begin{pmatrix} x \\ y \end{pmatrix} = \begin{pmatrix} 2\sum_{n=1}^{N} Xc_n^2 & 2\sum_{n=1}^{N} Xc_n \cdot Yc_n \\ 2\sum_{n=1}^{N} Xc_n \cdot Yc_n & 2\sum_{n=1}^{N} Yc_n^2 \end{pmatrix}^{-1} \begin{pmatrix} \sum_{n=1}^{N} (X2c_n + Y2c_n) \cdot Xc_n \\ \sum_{n=1}^{N} (X2c_n + Y2c_n) \cdot Yc_n \end{pmatrix} \quad (3.10)$$

where:

$$Xc_n = X_n - \frac{1}{N} \sum_{n=1}^{N} X_n \quad (3.11)$$

$$Yc_n = Y_n - \frac{1}{N} \sum_{n=1}^{N} Y_n \quad (3.12)$$

$$X2c_n = X_n^2 - \frac{1}{N} \sum_{n=1}^{N} X_n^2 \quad (3.13)$$

$$Y2c_n = Y_n^2 - \frac{1}{N} \sum_{n=1}^{N} Y_n^2 \quad (3.14)$$

Setting the x and y equations to zero in eq. (3.10), the centre of the Cole curve can be obtained. An example of the estimated centre of the circle is given in Figure 3.7.

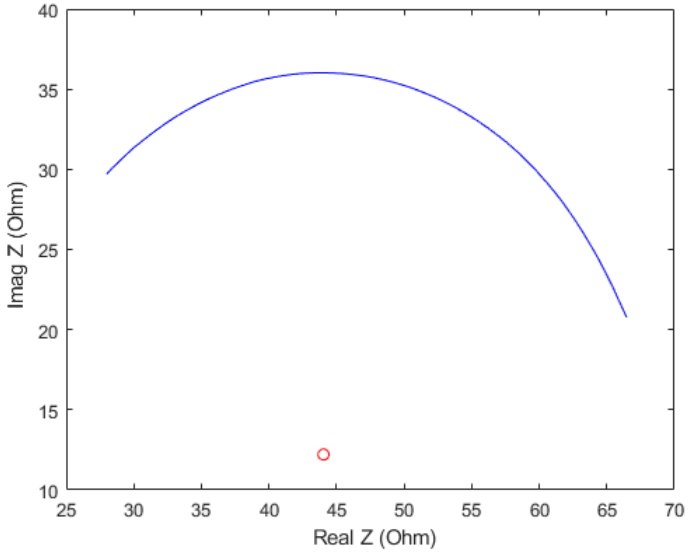

Figure 3.7: Coordinates of the centre of the circle (red point)

In detail, the real and imaginary parts (denoted as x and y respectively) of the centre of the circle and the radius R extracted from the Cole equation are:

$$x = \frac{R_0 + R_\infty}{2} \tag{3.15}$$

$$y = \frac{R_0 - R_\infty}{2} \cdot \frac{\cos(\alpha\pi/2)}{\sin(\alpha\pi/2)} \tag{3.16}$$

$$R = \frac{R_0 - R_\infty}{2\sin(\alpha\pi/2)} \tag{3.17}$$

Replacing the last result in equations (3.2) and (3.3), where $R(\omega) = \text{x}$ and $X(\omega) = \text{y}$, and combining them, R_0 and R_∞ can be found as:

$$R_\infty = x - \sqrt{R^2 - y^2} \tag{3.18}$$

$$R_0 = x + \sqrt{R^2 - y^2} \tag{3.19}$$

Moreover, the other two Cole-model parameters can be obtained from the slope that C - R_∞ has for $\alpha \leq 1$:

$$\alpha = 1 \pm \frac{2}{\pi} \cdot \phi \cdot \{C - R_\infty\} \tag{3.20}$$

therefore:

$$\alpha = 1 \pm \frac{2}{\pi} \cdot \arctan\left\{\left(\sqrt{\left(\frac{R}{y}\right)^2 - 1}\right)^{-1/2}\right\} \tag{3.21}$$

In this way, replacing α in the Cole equation (eq. 3.1) and solving it for τ, the value of f_c, i.e. the characteristic frequency, can be found as:

$$f_c = \frac{1}{\tau} \tag{3.22}$$

Finally, the fitting result and the output parameters of interest, i.e. R_0 and R_∞ (identified by green points), are shown in Figure 3.8.

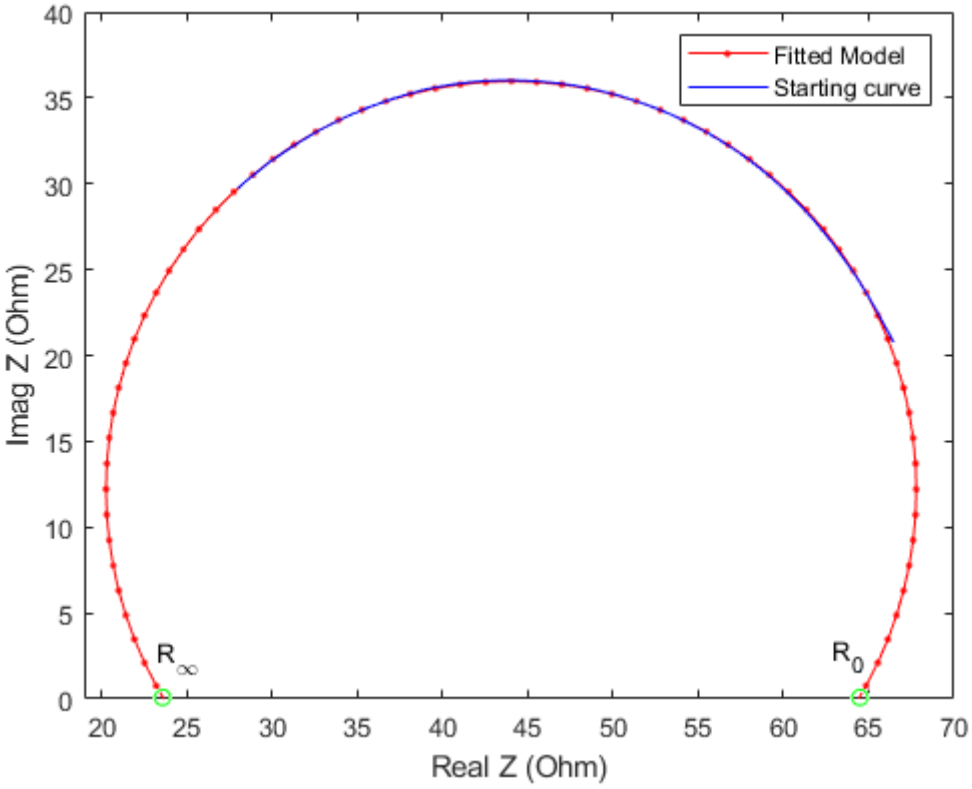

Figure 3.8: Superimposed curves: the blue line represents the bioimpedance measurement, at different frequencies, obtained from a specific body segment, while the red line is the result after processing by using the impedance plane fitting method

3.3.4 Body tissue characterization

After bioimpedance data collection, the R_0 and R_∞ parameters were estimated as explained by using the Impedance plane fitting method. As mentioned in Section 2.3.4, the resistance at zero frequency (R_0) corresponds to the extracellular resistance (R_{ECW}) because of the cell membrane's behaviour acting as an insulator at low frequencies. In contrast, the plasma membrane behaves like a good conductor at high frequencies, thus the current can pass through both ICF and ECF, and the resistance at infinity frequency (R_∞), which theoretically corresponds to the total body water resistance (R_{TBW}), can be found as indicated in equation (2.8). Therefore, taking advantage of having R_0 and R_∞ resistances, the intracellular resistance (R_{ICW}) can be estimated by reformulating eq. (2.8) as:

$$R_{ICW} = \frac{R_{TBW} \cdot R_{ECW}}{R_{ECW} - R_{TBW}} \tag{3.23}$$

Consequently, body tissues were characterized in terms of water contents and percentages of fat-free mass (FFM) and fat mass (FM). In fact, the equations (2.9), (2.10) and (2.11) were used to determine tissue contents such as ECW, ICW and TBW respectively, as well as the resistivity values reported in Table 2.2. It should be noted that the resistivities associated with the whole arm were used to estimate the ECW and ICW volumes of upper arms and forearms. This was made because these specific resistivity values were not found in the literature, but reasonable values have been obtained anyway. For the estimation of FM, different equations depending on different sexes have been used as reported in [14]:

$$M_{F_{male}} = -18.42 + 0.6 \cdot M_T - 0.57 \cdot \frac{H^2}{R_{TBW}} + 0.62 \cdot \frac{H^2}{R_{ECW}} \tag{3.24}$$

$$M_{F_{female}} = -9.81 + 0.65 \cdot M_T - 0.66 \cdot \frac{H^2}{R_{TBW}} + 0.65 \cdot \frac{H^2}{R_{ECW}} \tag{3.25}$$

where:

- M_T is the body weight;
- H is the subject's height;
- R_{TBW} and R_{ECW} are given as the sum of all the total body water and extracellular resistances considered from the different parts of the body.

To get an idea about the reliability of equations (3.24) and (3.25), a study for the estimation of FM considering 84 patients and 32 healthy subjects (for a total of 116 subjects) is reported in [53], where an FM overestimation of 6.55 $\pm$ 3.86 kg was found. Finally, the FFM can be easily calculated as the subtraction of the body weight and fat mass:

$$M_{FF} = M_T - M_F \tag{3.26}$$

In order to have a clear view of the implemented algorithm, the block diagram of the proposed method is shown in Figure 3.9.

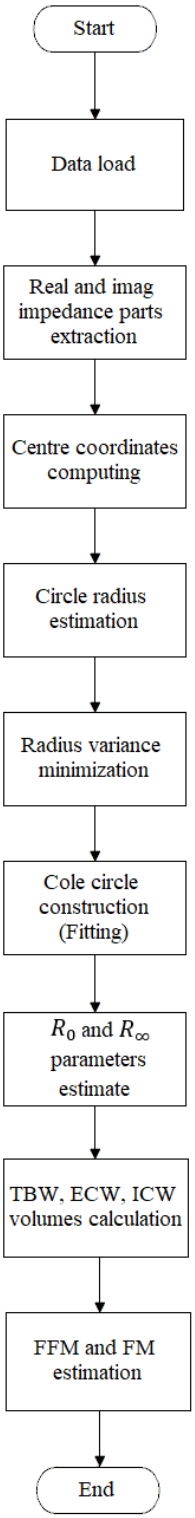

Figure 3.9: Block diagram of the proposed algorithm

3.4 Split Ring Resonator (SRR)

As previously mentioned, a further device was used to obtain additional parameters useful for a more complete characterization of biological tissues. This device is a split ring resonator (SRR) developed by the Microwaves in Medical Engineering Group (MMG) in Uppsala University (UU), and it is being studied in numerous medical applications such as orthopaedic monitoring and burn depth assessment [54], bone healing monitoring system for craniosynostosis patients [55], human tissue characterization [56]. A resonator is a system that exhibits resonance or resonant behaviour [57]. Different types of sensors were studied to design a proper SRR that could be adapted to be placed on the body [54]. Unlike other types of devices, the used microwave sensor is preferable for being small in size, comfortable, easy to use and extremely sensitive. It was developed to have the peak performance in the 2.4 GHz ISM (Industrial, scientific and medical) band which is free to use [58]. Moreover, the used SRR was chosen to be designed with a T-shape feeding (Figure 3.10) in order to have a good impedance matching to the body, high directivity (i.e. the measure of how well a system directs energy toward a particular direction), and a narrow bandwidth to distinguish resonance frequency shifts when connected to the area of interest [54]. More details regarding the SRR design can be found in [54].

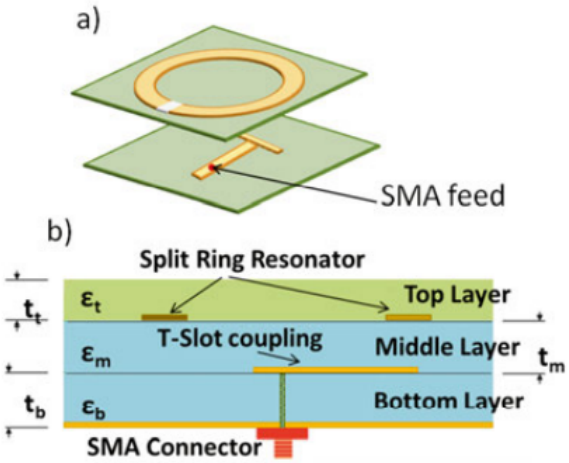

Figure 3.10: SRR design: a) T-shape feedline configuration; b) different layers of the structure [54]

In Figure 3.11 it can be seen the equivalent circuit for the SRR.

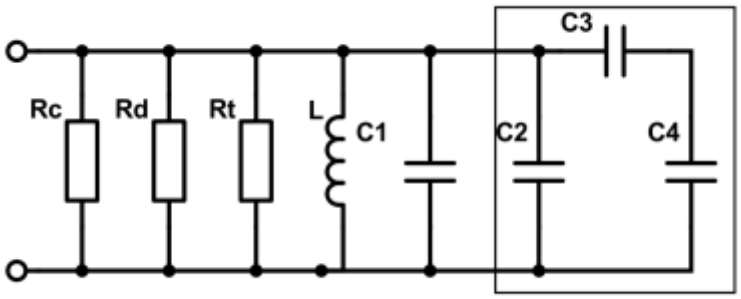

Figure 3.11: SRR equivalent circuit [55]

The SRR equivalent model is represented by a RLC parallel circuit, thus its transfer function is given as:

$$H(j\omega) = \frac{V_{out}}{V_{in}} = \frac{1}{j\omega C + \frac{1}{j\omega L} + \frac{1}{R}} \tag{3.27}$$

The SRR output data were collected by using a mini Vector Network Analyzer (mini-VNA Tiny version) which operates within a frequency range from 1 MHz to 3 GHz [59] (see Figure 3.12). The mini-VNA was used to send/receive microwave signals into/from the considered body segment so that the information could be stored and analysed on a pc that was set up to receive the data through USB cable.

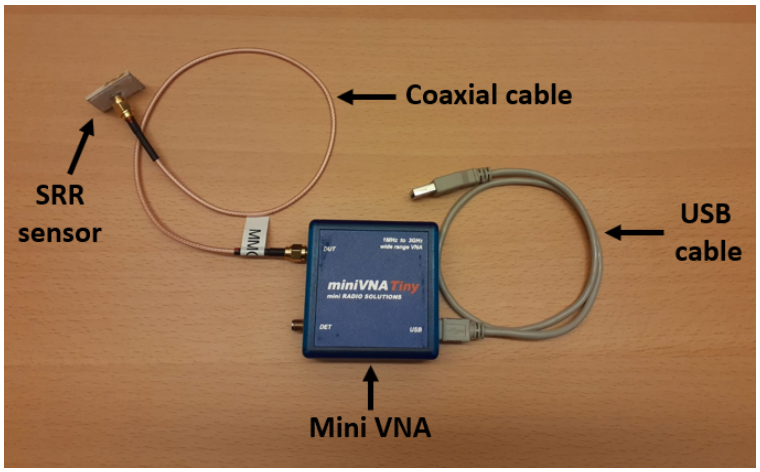

Figure 3.12: Hardware components used for measuring resonance frequency parameters

An example of how the SRR is applied to a specific body segment is given in Figure 3.13. For evaluating the measurement repeatability, three recordings have been conducted for each subject and each body segment and the average value of them has been used for the experiment.

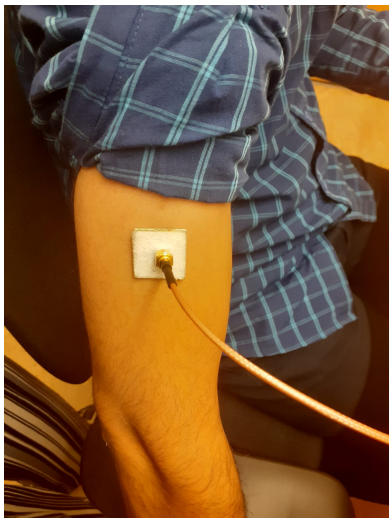

Figure 3.13: Application of SRR to the subject's upper arm for evaluating the resonance frequency parameters

However, based on the mentioned sensor specifications, the SRR output data have been used as a tool for understanding whether a body segment has more quantity of fat or muscle in a specific area (Figure 3.13). To intuitively analyse that, the reflection ($S11$) and transmission ($S21$) coefficients are investigated, where the former is the SRR output, while the latter is calculated as shown in equation (3.29). For the $S21$ calculation, V_I has been ideally considered equal to 1.

$$S11 = \frac{V_R}{V_I} \tag{3.28}$$

$$S21 = \frac{V_I - V_R}{V_I} \tag{3.29}$$

where

- V_R is the reflected voltage signal;
- V_I is the incident voltage signal.

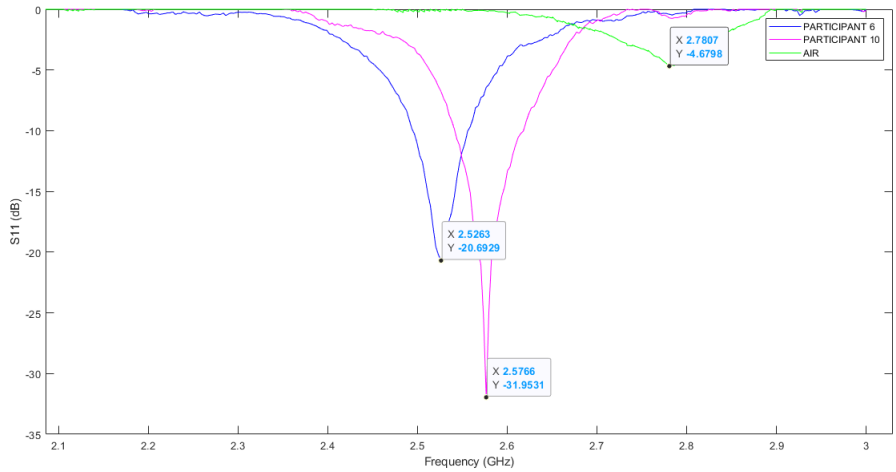

Figure 3.14: $S11$ of participants 6 and 10 (man and woman respectively) evaluated from their upper arms. The green line represents the $S11$ (in dB) obtained leaving the SRR in the air

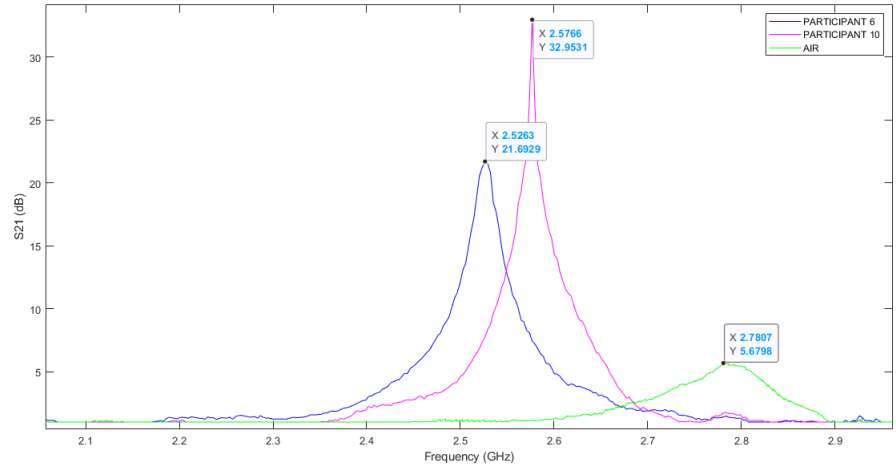

Figure 3.15: $S21$ of participants 6 and 10 (man and woman respectively) evaluated from their upper arms

The frequency that occurs at the peaks in the previous figures represents the resonance frequency, i.e. the frequency for which the antenna is able to absorb the maximum power from the transmission line. Considering the SRR output data in Figure 3.14, it can be seen that the resonant frequency amplitude associated with the upper arm of participant

6 (man) is about -20 dB, while it is around -32 dB for participant 10 (woman); therefore, the linear amplitudes (calculated by reformulating the equation 3.30) are 0.01 and 0.0005 respectively.

$$A_{dB} = 10 \cdot log(A) \tag{3.30}$$

where:

- A_{dB} is the amplitude in decibels;
- A is the linear amplitude.

Thus, participant 10 has a lower linear amplitude than participant 6. Moreover, the peak of resonant frequency f_R shifts more to the left (around 2.52 GHz) in the case of participant 6, while it shifts more to the right (around 2.57 GHz) in the case of participant 10, getting upwards to the free-space resonant frequency (around 2.8 GHz). This behaviour could be explained due to the lower dielectric properties of fat tissue compared to muscles [60] and also because, generally, women have higher percent body fat than men [61]. Furthermore, when an electromagnetic field is applied to the body, it penetrates more in fatty tissues because of their lower conductivity, due to the presence of lower water contents [62]. Against this background, peak values and resonance frequency shifts are analysed and correlations with the averaged bioimpedance moduli and the compressibility test are found.

3.5 Compressibility test

In addition to the bioimpedance and resonance frequency data collection, a study on the tissue compressibility is presented. The compressibility is defined as a measure of the relative volume change of a solid or fluid as a response to mean stress (or pressure) change [63]. Since the bioimpedance and the SRR output vary according to different body segment geometries, maximal and minimal circumferences were measured using a tape measure (Figure 3.16).

Figure 3.16: Circumference measurement by using a tape measure

The maximal circumference was evaluated without applying any pressure to the subject's district, in contrast the minimal circumference was measured encircling the body segment with more strength. As a result, the compressibility test was performed for each segment by calculating the delta Δ, expressed as percentage, as:

$$\Delta = \frac{Mc - mc}{Mc} \cdot 100 \ [\%] \tag{3.31}$$

where:

- Mc is the maximal circumference;
- mc is the minimal circumference.

In this thesis, the compressibility test is used to better understand the information obtained from the bioimpedance data and the resonance parameters. Indeed, taking into account that fatty tissues have stiffer (more rigid) material properties [64, 65], some correlations among these data will be shown in the next Chapter in order to comprehend what type of tissue is being analysed.

Chapter 4

Results and Discussion

In this Chapter, parameters useful for the body tissue characterization extracted as previously described, are presented. In particular, the body segments suitable for the application of the disposable patch are considered, each of which is characterized in terms of:

- bioimpedance moduli;
- R_{ECW}, R_{TBW} and R_{ICW} resistances of body fluids;
- ECW, ICW, TBW volumes;
- tissue compressibility;
- resonance parameters.

Furthermore, it is considered that the human body is composed of two main compartments, i.e. fat and lean components. Therefore, FFM and FM are also computed. Particularly, FFM, being composed of bone tissue and body cell mass (included skeletal tissue and proteins) provides information about such components [14]. Finally, validation of the algorithm results is performed. It is important to note that, as standard techniques such as DXA, MRI, and CT are quite unhandy and costly, the obtained parameters are validated by comparing the data found in the literature. What the compressibility test and the SRR output data provide to this work is additional information about the fat and lean contents of a specific body segment.

4.1 Bioimpedance moduli

As previously mentioned in Section 3.2, an important observation was that acquiring bioimpedance signals from the right side of the body or from the left side resulted in minimal differences. This was proved only on three subjects from which the average bioimpedance data reported in Table 4.1 were collected.

Body segment	**Subjects**	**Z - Right side (Ω)**	**Z - Left side (Ω)**
CHEST	2	63.25	64.87
	4	110.76	108.84
	9	58.79	59.86
UPPER ARM	2	65.88	67.02
	4	89.52	87.64
	9	91.50	90.14
FOREARM	2	59.35	59.21
	4	60.06	58.64
	9	54.05	54.62
LEG	2	66.40	67.29
	4	58.34	55.87
	9	120.53	118.76

Table 4.1: Average values of bioimpedance moduli from the right and left sides of the body

Due to the similar results, only the right side of the body was chosen to be analysed in order to make the procedure less time-consuming. However, the complete dataset of bioimpedance signals has been collected from 10 participants, whose physical characteristics are reported in Table 3.1. Average values of bioimpedance moduli, expressed in ohm, are reported in Table 4.2 and shown in Figure 4.1 for each subject.

Body segment	Subjects	Z (Ω)
CHEST	1	75.98
	2	63.25
	3	65.86
	4	110.76
	5	89.27
	6	93.79
	7	70.43
	8	96.56
	9	58.79
	10	88.29
	AVERAGE	**81.30**
	ST_DEV	**16.95**
UPPER ARM	1	73.70
	2	65.88
	3	80.11
	4	89.52
	5	75.57
	6	65.90
	7	79.95
	8	90.84
	9	91.50
	10	121.34
	AVERAGE	**83.43**
	ST_DEV	**16.29**
FOREARM	1	63.21
	2	59.35
	3	82.35
	4	60.06
	5	76.03
	6	45.43
	7	58.90
	8	71.73
	9	54.05
	10	86.73
	AVERAGE	**65.78**
	ST_DEV	**13.05**
LEG	1	43.45
	2	66.40
	3	70.33
	4	58.34
	5	50.15
	6	46.34
	7	74.31
	8	83.57
	9	120.53
	10	104.21
	AVERAGE	**71.76**
	ST_DEV	**25.17**

Table 4.2: Average values of bioimpedance moduli from different body districts

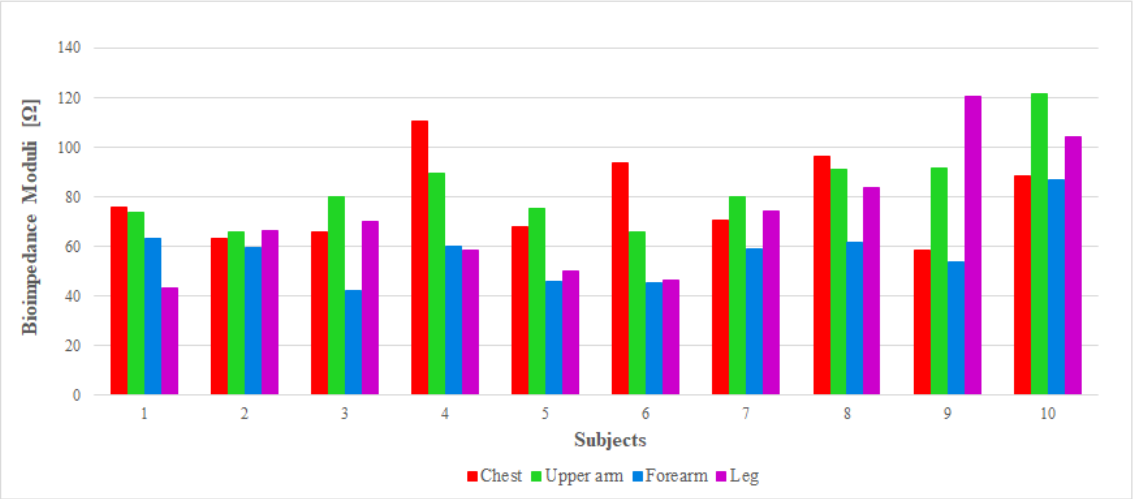

Figure 4.1: Bioimpedance moduli acquired from different parts of the body

It is observed that the bioimpedance values range from 43.44 Ω up to 121.33 Ω. It is possible to make a comparison with some of the analyzed areas, especially chest and upper arm, with values found in the literature. Figure 4.2 shows typical impedance values [66] collected from different body segments.

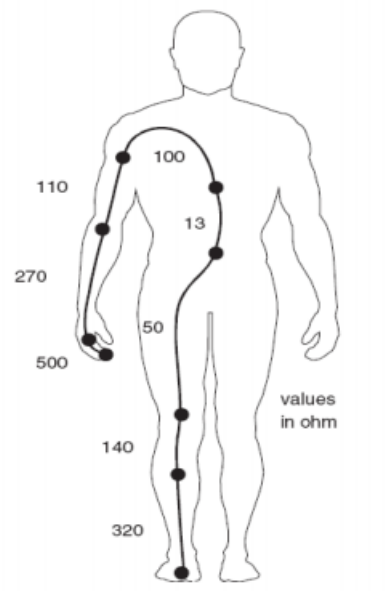

Figure 4.2: Typical bioimpedance values

For the case of chest and upper arm, the average impedance moduli obtained in the present study are 81.30 ± 25.98 Ω and 83.42 ± 27.73 Ω respectively. Based on the considerations given in Section 2.2 that the bioimpedance measurements depend on different factors, the collected average values could be considered reasonable because they are quite similar to the reference values which are about 113 and 110 Ω for chest and upper arm respectively. Other bioimpedance data associated to the subjects' forearms and lower legs cannot be compared because of the different location of the electrodes which cover a different area of interest. However, these bioimpedance moduli data will be included in the further study described in Section 4.5.

4.2 Characteristic resistance values

By using the impedance plane fitting method, the R_{ECW}, R_{TBW} and R_{ICW} parameters have been estimated and successively compared with the ones reported in [67]. The three extracted resistances are reported in Table 4.3.

Body segment	Subjects	$R_{ECW}(\Omega)$	$R_{TBW}(\Omega)$	$R_{ICW}(\Omega)$
CHEST	1	68.37	31.64	58.90
	2	50.11	30.07	75.20
	3	72.35	28.95	48.26
	4	127.85	39.40	56.94
	5	61.22	26.02	45.24
	6	82.21	43.58	92.76
	7	63.47	31.14	61.13
	8	82.08	24.27	34.47
	9	52.37	19.48	31.03
	10	83.32	16.53	20.62
	AVERAGE	**74.33**	**29.11**	**52.45**
	ST_DEV	**22.27**	**8.24**	**21.46**
UPPER ARM	1	93.36	31.28	46.31
	2	84.01	37.59	68.04
	3	84.60	33.58	55.67
	4	112.04	29.72	40.46
	5	94.49	36.17	58.60
	6	84.19	35.05	60.06
	7	99.24	39.14	64.62
	8	148.62	31.70	40.29
	9	111.33	37.66	56.92
	10	150.80	33.89	43.71
	AVERAGE	**106.57**	**34.58**	**53.47**
	ST_DEV	**24.89**	**3.10**	**10.07**
FOREARM	1	80.59	37.27	69.32
	2	61.95	35.18	81.40
	3	60.19	23.41	38.31
	4	76.57	35.37	65.73
	5	52.93	27.31	56.43
	6	62.05	34.36	77.02
	7	80.51	32.32	53.99
	8	82.34	26.30	38.64
	9	72.77	31.69	56.15
	10	97.16	28.57	40.48
	AVERAGE	**72.71**	**31.18**	**57.75**
	ST_DEV	**13.36**	**4.57**	**15.59**
LEG	1	63.02	25.99	44.23
	2	87.34	29.88	45.42
	3	75.51	30.65	51.58
	4	74.51	33.92	62.28
	5	68.67	32.23	60.73
	6	63.83	25.67	42.94
	7	93.22	37.92	63.92
	8	98.12	50.21	102.83
	9	140.71	60.59	106.41
	10	106.78	47.70	86.21
	AVERAGE	**87.17**	**37.48**	**66.66**
	ST_DEV	**23.98**	**11.63**	**23.75**

Table 4.3: Estimated R_{ECW}, R_{TBW} and R_{ICW} from subjects' chest, upper arm, forearm and leg

In order to have a clearer picture of the estimated data, the R_{ECW}, R_{TBW} and R_{ICW} parameters are plotted using line graphs (see Figure 4.3).

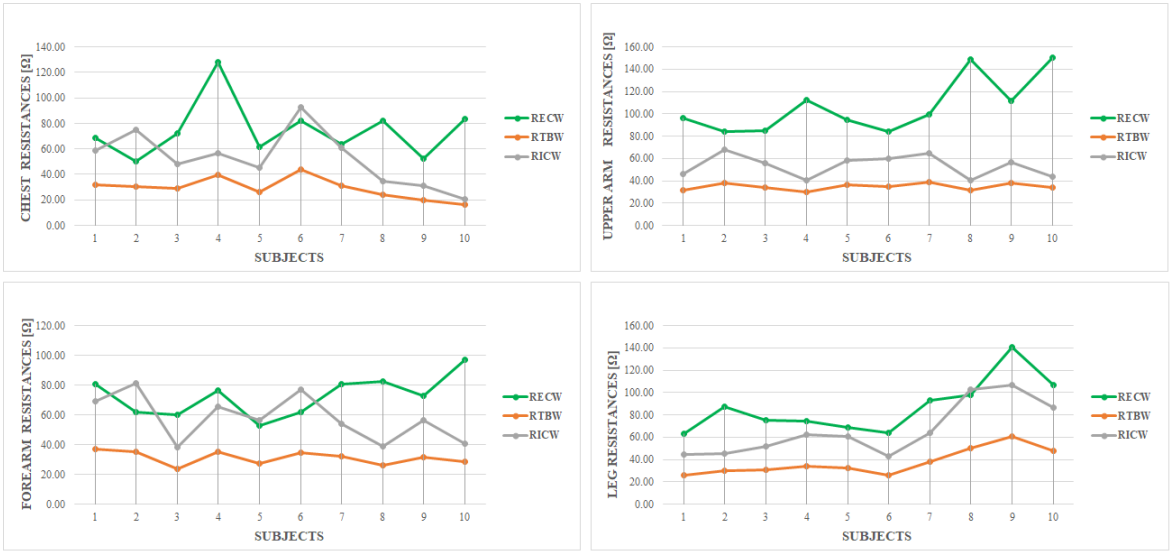

Figure 4.3: Estimated resistances for each body segment: R_{ECW} (green), R_{TBW} (orange) and R_{ICW} (grey)

As previously mentioned, reference values of R_{ECW} and R_{ICW} resistances are found in [67] where a study on 15 subjects (7 males with an average age of 23.86 $\pm$ 1.46, 8 females with an average age of 24.50 $\pm$ 2.560) was performed. An important observation is that the anthropometric characteristics of the subjects (averaged height of 1.78 $\pm$ 0.04 m and averaged weight of 72.36 $\pm$ 8.63 kg) involved in [67] are similar to those involved in the present study with an average age of 26.30 $\pm$ 11.50 years, average weight of 65.52 $\pm$ 22.6 kg and average height of 170.50 $\pm$ 15 cm, as indicated in Table 3.1 which is reported again below to facilitate the reader's understanding.

Participant	Sex	Age	Weight [kg]	Height [cm]
1	Male	35	50.3	158
2	Male	24	62	174
3	Male	25	62.4	165.5
4	Male	39	95.5	178
5	Male	23	64.7	166.5
6	Male	24	70	172
7	Male	16	67.7	188
8	Female	24	70	172
9	Female	21	55	170
10	Female	32	57.7	161
AVERAGE	/	**26.30**	**65.52**	**170.50**
ST_DEV	/	**6.93**	**12.34**	**8.61**

Table 3.1: Characteristics of the participants

Moreover, since the experiment in [67] was performed by evaluating the overall arm (not upper arms and forearms separately), the collected R_{ECW} and R_{ICW} of the subjects' forearms and upper arms were added in order to make comparisons between them (see Table 4.5 and Figure 4.4). This assumption was chosen to be used with the arm resistance considered as the result of series resistances of upper arm and forearm.

Body segment	Subjects	$R_{ECW}(\Omega)$	$R_{TBW}(\Omega)$	$R_{ICW}(\Omega)$
ARM	1	176.95	68.54	115.62
	2	145.97	72.77	149.44
	3	144.79	56.99	93.98
	4	188.61	65.09	106.19
	5	147.42	63.48	115.03
	6	146.24	69.42	137.07
	7	179.75	71.45	118.60
	8	230.97	58.00	78.94
	9	184.10	69.36	113.06
	10	247.96	62.46	84.19
	AVERAGE	**179.28**	**65.76**	**111.21**
	ST_DEV	**36.38**	**5.47**	**21.90**

Table 4.5: Estimated R_{ECW}, R_{TBW} and R_{ICW} from subjects' arm

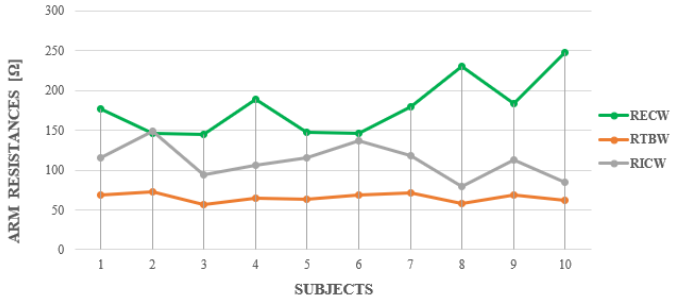

Figure 4.4: Arm resistances: R_{ECW} (green), R_{TBW} (orange) and R_{ICW} (grey)

Having done this, average reference values and the ones estimated in this work are indicated in Tables 4.6 and 4.7 respectively. In this way, some comparisons can be made.

	Trunk	**Arm**	**Leg**
$R_{ECW}(\Omega)$	76.64 ± 10.76	311.60 ± 36.70	268.11 ± 31.90
$R_{ICW}(\Omega)$	96.78 ± 16.09	758.35 ± 182.66	594.18 ± 129.27

Table 4.6: Reference resistance values reported in [67]

	Trunk	**Arm**	**Leg**
$R_{ECW}(\Omega)$	74.33 ± 38.87	179.28 ± 51.50	87.17 ± 43.44
$R_{ICW}(\Omega)$	52.45 ± 36.07	111.21 ± 35.00	66.66 ± 42.15

Table 4.7: Estimated R_{ECW} and R_{ICW}

Observing ECW and ICW resistances of chest, it can be noted that the averaged values of R_{ECW} are not so different from the reference values, while R_{ICW} values are almost halved. As regards the ECW and ICW resistances of arm, a relevant difference can be noted between the reference values and the ones estimated in the present study. In particular, the estimated R_{ECW} of arm is almost half of the referenced R_{ECW} of arm. Finally, the R_{ECW} and R_{ICW} resistances are different and this can be associated with the fact that only the lower leg was analyzed in this research study.

4.3 TBW, ECW, ICW volumes

The extraction of the previous parameters has carried out the characterization of TBW, ECW, ICW volumes associated with the considered body districts. These results are reported in Table 4.8 and plotted in Figure 4.5:

Body segment	**Subjects**	**Length (cm)**	**ECW** (kg)	**ICW** (kg)	**TBW** (kg)
CHEST	1	44.50	4.61	8.41	13.01
	2	53.50	9.08	9.52	18.60
	3	52.00	5.94	14.01	19.05
	4	61.50	4.70	16.61	21.31
	5	51.50	6.89	14.66	21.54
	6	53.00	5.43	7.57	13.00
	7	59.50	8.87	14.48	23.35
	8	54.00	6.11	22.50	28.61
	9	51.50	8.71	22.74	31.45
	10	46.00	4.37	27.30	31.67
	AVERAGE	**52.70**	**6.47**	**15.78**	**22.25**
	ST_DEV	**5.18**	**1.83**	**6.62**	**6.72**
UPPER ARMS	1	34.50	0.83	2.49	3.32
	2	34.50	0.95	1.70	2.65
	3	35.50	1.00	2.20	3.19
	4	34.50	0.71	2.85	3.57
	5	34.00	0.82	1.91	2.73
	6	31.00	0.76	1.55	2.32
	7	37.50	0.95	2.11	3.06
	8	35.50	0.57	2.99	3.55
	9	38.50	0.89	2.49	3.38
	10	35.00	0.54	2.68	3.22
	AVERAGE	**35.05**	**0.80**	**2.30**	**3.10**
	ST_DEV	**2.02**	**0.16**	**0.48**	**0.41**
FOREARM	1	23.50	0.46	0.77	1.23
	2	28.00	0.85	0.93	1.78
	3	24.50	0.67	1.52	2.19
	4	23.50	0.48	0.81	1.30
	5	24.00	0.73	0.99	1.72
	6	27.00	0.79	0.92	1.71
	7	28.70	0.69	1.48	2.17
	8	25.50	0.53	1.61	2.14
	9	25.50	0.60	1.11	1.70
	10	23.00	0.36	1.25	1.61
	AVERAGE	**25.32**	**0.62**	**1.14**	**1.75**
	ST_DEV	**2.00**	**0.16**	**0.31**	**0.34**
LEG	1	36.50	1.04	4.23	5.27
	2	40.00	0.90	4.95	5.85
	3	38.00	0.94	3.93	4.87
	4	45.50	1.36	4.67	6.03
	5	38.50	1.06	3.43	4.49
	6	42.00	1.35	5.77	7.13
	7	50.50	1.34	5.61	6.95
	8	44.00	0.98	2.65	3.62
	9	45.50	0.73	2.73	3.46
	10	39.00	0.71	2.48	3.18
	AVERAGE	**41.95**	**1.04**	**4.04**	**5.08**
	ST_DEV	**4.37**	**0.24**	**1.21**	**1.41**

Table 4.8: Estimated ECW, ICW and TBW from subjects' chest, upper arm, forearm and leg

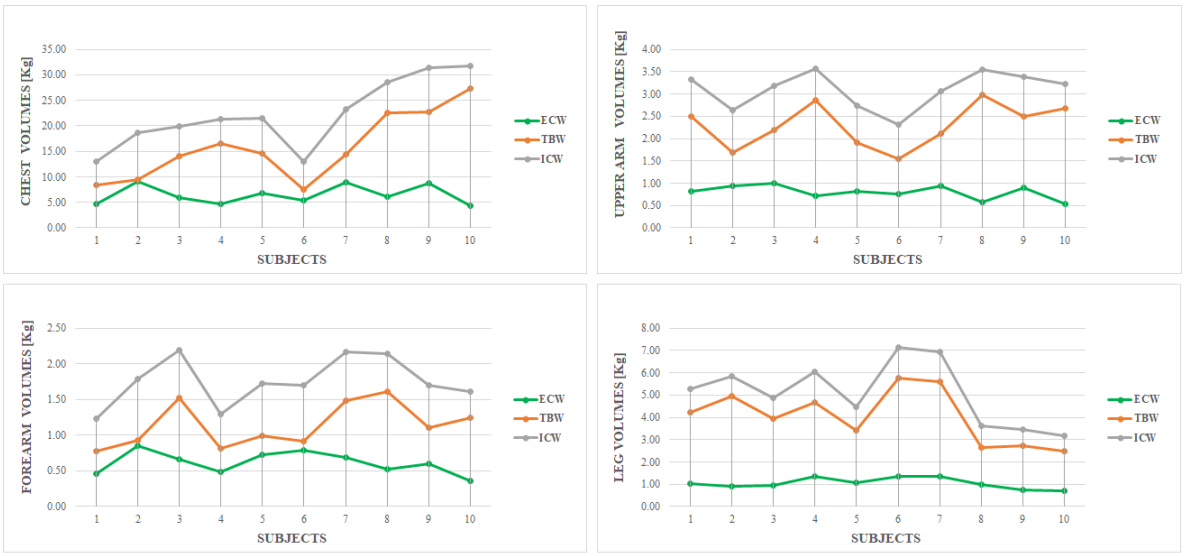

Figure 4.5: Volumes for each body segment analyzed: ECW in green, TBW in orange and ICW in grey

In the same way as the resistance parameters are calculated, also the ECW, ICW and TBW volumes of the arm are defined as the sum of upper arm and forearm volumes (see Table 4.9 and Figure 4.6). It is important to observe that the specific resistivities of arms and legs, reported in 2.2, have been halved because the considered segments are upper arms, forearms and lower legs.

Body segment	Subjects	ECW (kg)	ICW (kg)	TBW (kg)
ARM	1	1.29	3.27	4.55
	2	1.80	2.63	4.43
	3	1.67	3.72	5.38
	4	1.20	3.67	4.86
	5	1.55	2.90	4.45
	6	1.55	2.47	4.02
	7	1.63	3.59	5.23
	8	1.10	4.59	5.69
	9	1.49	3.59	5.08
	10	0.91	3.92	4.83
	AVERAGE	**1.42**	**3.44**	**4.85**
	ST_DEV	**0.28**	**0.64**	**0.51**

Table 4.9: Estimated ECW, ICW, TBW from subjects' arm

Figure 4.6: Arm volumes: ECW (green), TBW (orange) and ICW (grey)

The same paper [67] is considered to compare ECW and ICW volumes. The reference and estimated values are reported in Tables 4.10 and 4.11 respectively. TBW volumes are also compared as it is the sum of ECW and ICW.

	Trunk	**Arm**	**Leg**
ECW (kg)	10.46 ± 1.44	0.70 ± 0.12	1.83 ± 0.14
ICW (kg))	19.02 ± 2.34	1.04 ± 0.30	2.57 ± 0.18

Table 4.10: Reference volumes reported in [67]

	Trunk	**Arm**	**Leg**
ECW (kg)	6.47 ± 2.35	1.42 ± 0.44	1.04 ± 0.32
ICW (kg))	15.78 ± 9.86	3.44 ± 1.06	4.04 ± 1.64

Table 4.11: Estimated ECW and ICW

For the water volumes of chest, it can be seen that estimated values are very similar to the literature results. Regarding the ECW and ICW volumes of arms and legs, the former are quite comparable with the respect of the reference values, on the other hand, the latter results are very different. Further considerations can be done considering specific percentage values representing the overall human body weight (Figure 4.7). With the aim of validating the obtained results still further, the mean absolute error e was calculated as:

$$e = \frac{1}{N} \sum_{n=1}^{N} |x - y| \tag{4.1}$$

where:

- N is the number of the calculated errors;

- x is the reference value reported in Figure 4.7;
- y is the estimated value.

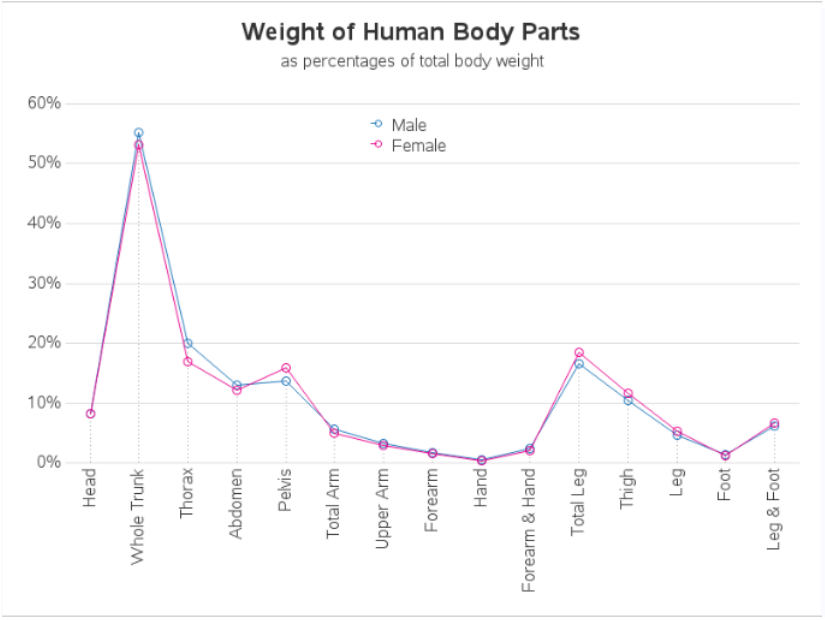

Weight of Human Body Parts as percentages of total body weight

Segment	Male	Female
Head	8.26%	8.20%
Whole Trunk	55.1%	53.2%
Thorax	20.1%	17.0%
Abdomen	13.1%	12.2%
Pelvis	13.7%	16.0%
Total Arm	5.70%	4.97%
Upper Arm	3.25%	2.90%
Forearm	1.87%	1.57%
Hand	0.65%	0.50%
Forearm & Hand	2.52%	2.07%
Total Leg	16.7%	18.4%
Thigh	10.5%	11.8%
Leg	4.75%	5.35%
Foot	1.43%	1.33%
Leg & Foot	6.18%	6.68%

Figure 4.7: Weight of human body parts [68]

In general, as it can be seen from Figure 4.7, the weight of total arm for male and female corresponds respectively to 5.70 % and 4.97 % of the total body weight. Considering the average of these two percentage values (which is 5.34 %) and the average weight of 62.52 kg, it is expected to obtain approximately an average weight of total arm for both sexes of 3.34 kg, whereas a value of 4.86 kg is reached. This value is obtained as the sum of 1.42 and 3.44 (which are the ECW and ICW arm values reported in Table 4.9) and, therefore, a mean absolute error of 1.52 kg is found. Similarly, legs are about 4.75 % and 5.35 % of the total body weight for male and female respectively, thus an average percentage of 5.05 % can be roughly considered. In this case, a mean absolute error of 1.95 kg is found since the obtained value is about 5.08 kg (addition of ECW and ICW leg volumes), while the expected one is about 3.13 kg (calculated as 5.05 % of the average total body weight).

4.4 FFM and FM results

Commercial devices (some of which are reported in Table 2.3) can estimate FFM and FM of specific body segments using regression techniques [69]. However, since the majority

of papers in the literature mention that FFM and FM are estimated considering the whole body, such parameters have been determined in this way. As mentioned in Section 3.3.4, FM and FFM are computed by including the total R_{ECW} and R_{TBW} parameters indicated in Table 4.12.

Subjects	$R_{ECW}(\Omega)$	$R_{TBW}(\Omega)$
1	548.32	220.71
2	516.71	235.37
3	512.96	204.22
4	654.09	237.43
5	493.39	217.43
6	502.34	233.75
7	609.43	249.88
8	740.25	240.69
9	702.00	279.38
10	792.79	236.85
AVERAGE	**607.23**	**235.57**
ST_DEV	**109.45**	**20.25**

Table 4.12: Estimation of the total R_{ECW} and R_{TBW}

Therefore, using the equations (3.24) and (3.25), the obtained values of FM and FFM are reported in Table 4.13.

Subjects	**FM (kg)**	**FFM (kg)**
1	11.40	38.90
2	18.41	43.59
3	18.59	43.81
4	38.42	57.08
5	20.02	44.68
6	23.22	46.78
7	21.69	45.91
8	35.14	34.86
9	25.52	29.48
10	27.19	30.51
AVERAGE	**23.96**	**41.56**
ST_DEV	**8.07**	**8.34**

Table 4.13: FM and FFM estimation

By analyzing Table 4.13, it can be noted that the lowest and highest values of FM (which are 11.40 and 38.40 kg respectively) correspond to the participants whose weights

are respectively the lowest and highest with 50.3 kg for participant 1 and 95.5 for participant 4. This demonstrates that a strong link between the subjects' weight and the obtained FM values is found and, in particular, as weight increases, FM increases as well. FM and FFM can also be analyzed in the form of histograms as shown in Figure 4.8.

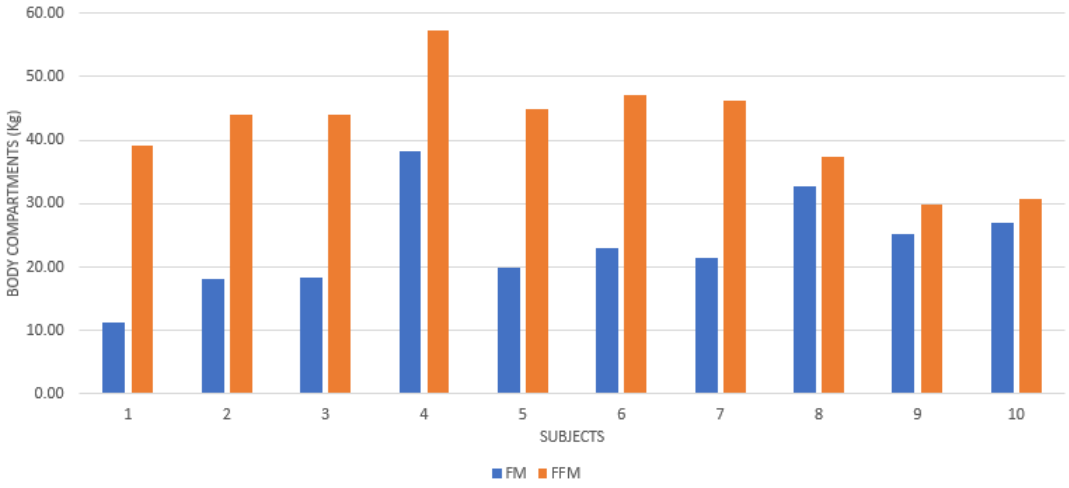

Figure 4.8: Body compartments distribution: FM (blue) and FFM (orange)

The obtained average FM is equal to 23.96 ± 13.51 kg, while the average FFM is 41.56 ± 13.80 kg. Reference values of these parameters are found in [70], where FM and FFM are equal to 27.66 ± 0.60 kg and 45.94 ± 0.76 kg respectively. In the study reported in [70], the dataset consisted of subjects with different average age, but very similar anthropometric characteristics. However, mean absolute errors of 3.7 kg for FM and 4.38 kg for FFM are obtained.

4.5 Compressibility and Resonance Parameters

Compressibility and resonance parameters have been used as supplementary information for the characterization of tissue contents, as well as valuable evaluation tool. Table 4.14 shows the results of the compressibility test (i.e. the delta calculation), and the maximum and minimum circumferences measured from different body segments.

Body segment	Subjects	Mc (cm)	mc (cm)	Δ (%)
CHEST	1	76.50	73.00	4.57
	2	90.50	86.50	4.42
	3	86.50	83.50	3.47
	4	108.50	105.50	2.76
	5	103.50	101.30	2.16
	6	91.50	88.70	3.06
	7	84.50	81.50	3.55
	8	94.50	91.50	3.17
	9	84.30	81.30	3.56
	10	86.50	83.50	3.47
	AVERAGE	**90.68**	**87.63**	**3.42**
	ST_DEV	**9.50**	**9.71**	**0.71**
UPPER ARM	1	23.70	22.70	4.22
	2	26.50	24.80	6.42
	3	26.80	26.00	2.98
	4	31.50	30.50	3.17
	5	31.50	30.00	4.84
	6	30.50	29.00	4.92
	7	25.50	24.50	3.92
	8	28.00	27.50	1.78
	9	25.20	23.80	5.56
	10	22.50	21.50	4.44
	AVERAGE	**27.17**	**26.03**	**4.23**
	ST_DEV	**3.17**	**3.11**	**1.34**
FOREARM	1	17.30	16.50	4.57
	2	18.50	17.20	7.03
	3	20.00	19.30	3.50
	4	21.40	20.50	4.21
	5	24.00	23.30	2.92
	6	25.40	24.40	3.88
	7	18.10	17.40	3.87
	8	18.70	18.20	2.67
	9	22.50	21.80	3.15
	10	17.00	16.50	2.94
	AVERAGE	**20.29**	**19.51**	**3.87**
	ST_DEV	**2.91**	**2.87**	**1.27**
LEG	1	29.50	28.10	4.75
	2	32.60	31.80	2.45
	3	32.10	31.40	2.18
	4	32.10	30.20	5.92
	5	33.50	32.20	3.85
	6	34.50	33.40	3.19
	7	30.70	29.50	3.91
	8	32.50	31.50	3.07
	9	30.50	29.50	3.28
	10	25.50	24.50	3.92
	AVERAGE	**31.35**	**30.20**	**3.65**
	ST_DEV	**2.53**	**2.52**	**1.10**

Table 4.14: Averaged values of bioimpedance moduli from different body districts

The data obtained from the compressibility test can also be analyzed in the histogram in Figure 4.9:

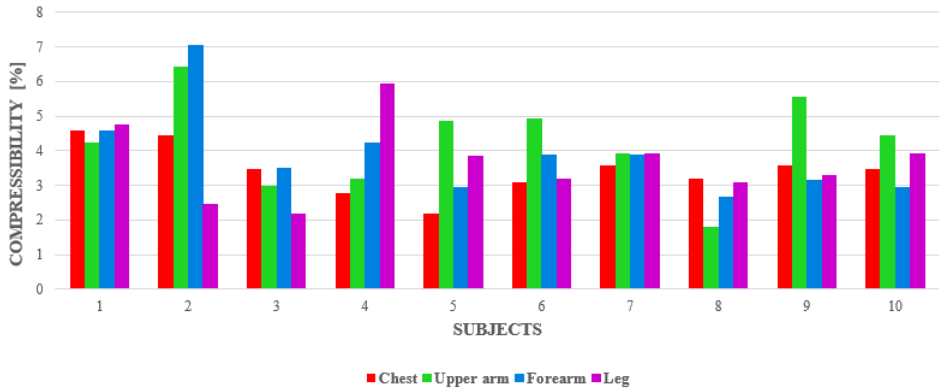

Figure 4.9: Compressibility test

As it can be observed from Figure 4.9, the compressibility of all body tissues is higher than 2 % except the one of participant 8 whose upper arm compressibility is lower. Taking a closer look at the histogram, participants 2 and 9 show an upper arm compressibility larger than 5 %, and this results in a lower fat content in the specific area. This is also due to the higher elasticity of the considered segment. Another example can be made considering subject 8 who has the lowest forearm compressibility. Similar considerations could be made for the other participants data.

The collected resonance data are instead reported in Table 4.15 and plotted in Figure 4.10.

Body segment	**Subjects**	**f$_R$(GHz)**	**Amplitude (dB)**	**Phase** (deg)
CHEST	1	2.499	-14.563	-150.613
	2	2.517	-20.107	-146.178
	3	2.517	-15.149	-135.294
	4	2.542	-24.144	-162.855
	5	2.533	-22.472	-140.387
	6	2.512	-18.795	-150.637
	7	2.517	-17.651	-153.291
	8	2.514	-16.344	-135.810
	9	2.509	-18.384	-135.820
	10	2.520	-18.983	-131.814
	AVERAGE	**2.518**	**-18.659**	**-144.269**
	ST_DEV	**0.012**	**3.026**	**10.028**
UPPER ARM	1	2.544	-33.602	-109.442
	2	2.514	-20.840	-161.474
	3	2.562	-36.004	-154.467
	4	2.532	-25.923	-131.043
	5	2.529	-29.317	-142.916
	6	2.526	-20.693	-139.818
	7	2.606	-28.127	-165.847
	8	2.586	-39.576	-157.444
	9	2.547	-33.586	-157.445
	10	2.577	-21.802	-152.953
	AVERAGE	**2.552**	**-28.947**	**-147.285**
	ST_DEV	**0.030**	**6.674**	**17.019**
FOREARM	1	2.514	-14.439	-146.988
	2	2.499	-14.121	-174.322
	3	2.636	-17.558	-162.428
	4	2.526	-16.783	-143.413
	5	2.559	-27.575	-129.600
	6	2.532	-16.463	-133.510
	7	2.523	-17.477	-143.753
	8	2.562	-29.940	-142.897
	9	2.523	-15.920	-142.890
	10	2.556	-27.015	-167.477
	AVERAGE	**2.543**	**-19.731**	**-148.729**
	ST_DEV	**0.039**	**5.980**	**14.590**
LEG	1	2.514	-14.549	-162.931
	2	2.544	-36.987	-134.479
	3	2.562	-34.725	-137.913
	4	2.526	-22.806	-156.500
	5	2.538	-19.278	-132.261
	6	2.541	-30.328	-144.071
	7	2.553	-47.761	-76.686
	8	2.550	-41.157	-56.596
	9	2.565	-37.166	-56.596
	10	2.532	-37.463	-174.578
	AVERAGE	**2.543**	**-32.222**	**-123.261**
	ST_DEV	**0.016**	**10.405**	**43.747**

Table 4.15: Resonance frequency data obtained with the SRR

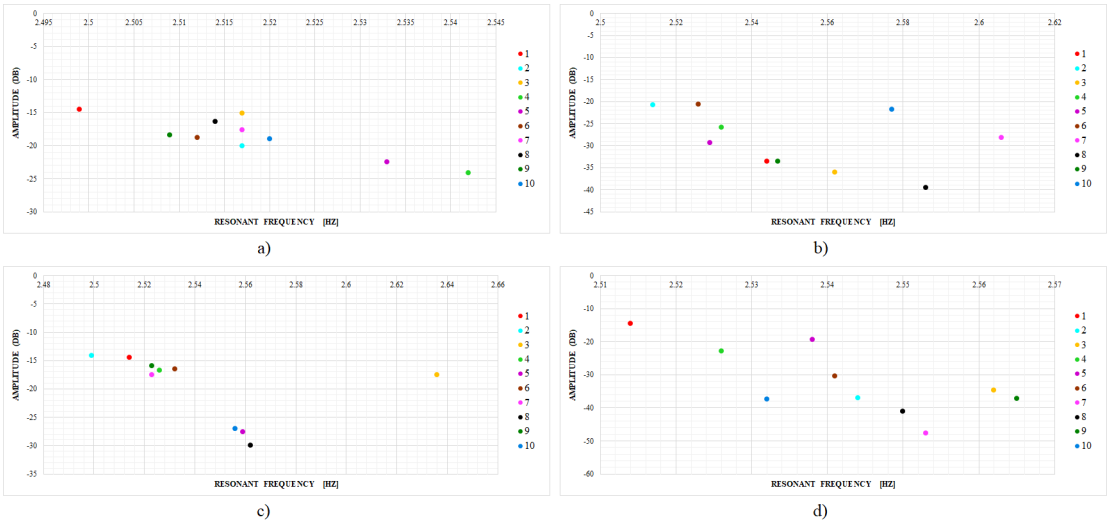

Figure 4.10: Amplitude and resonant frequency data evaluated from different body segments: a) chest; b) upper arm; c) forearm; d) lower leg

Observing Figure 4.10 a, it can be noticed that the majority of peaks are concentrated within a frequency range between 2.51 and 2.52 GHz except participants 1, 4 and 5. Considering participants 1 and 4, the resonant frequency peaks are at about 2.50 GHz and 2.54 GHz and amplitude of about -14 dB and -24 dB are found respectively. According to the considerations mentioned in Chapter 3, participant 1 has a lower fat content than participant 4. Moreover, this can be reflected with respect to the average bioimpedance moduli which are about 75 Ω and 110 Ω for participants 1 and 4 respectively. Similar considerations can be made for the other involved participants and for each body segment.

In addition, the next section describes the implementation of a clustering algorithm. This is done to evaluate whether it is possible to find a correspondence between the anthropometric characteristics and the dataset that includes bioimpedance, compressibility and resonance parameters.

4.6 Clustering algorithm

A k-means clustering method is implemented to cluster and distinguish the data in different groups using MATLAB®. Such method was performed using the MATLAB®function called $k - means$, which is based on a squared Euclidean distance metric, bringing into play the bioimpedance moduli, the resonance parameters and the result of the compressibility test. By looking at the subjects' weight, three clusters have been chosen for the implementation of the k-means algorithm. Results of this method can be seen in Figure 4.11 and 4.12.

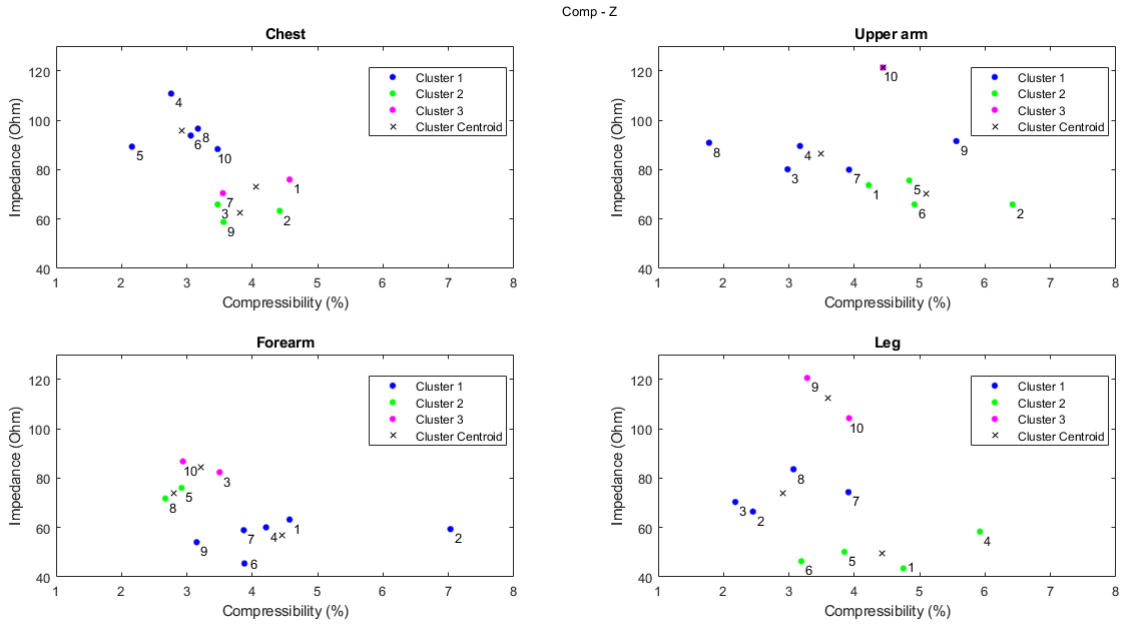

Figure 4.11: k-means output: Impedance versus Compressibility

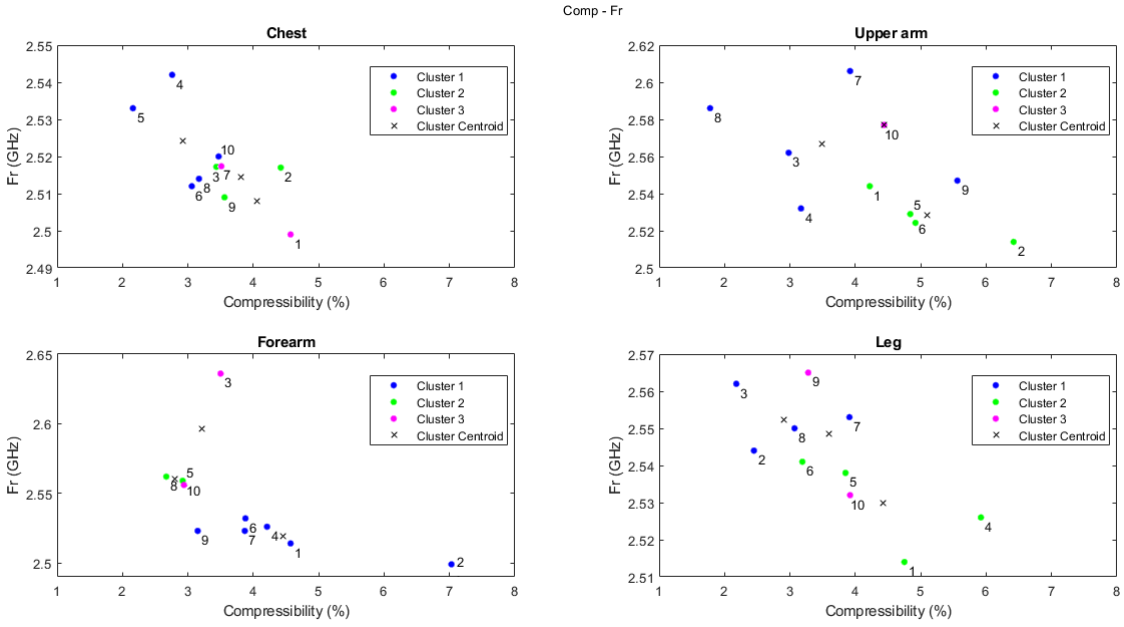

Figure 4.12: k-means output: Resonance frequency versus Compressibility

From the obtained results, the participants are grouped into three different clusters. An interesting concept that can be investigated is what participants, belonging in a specific cluster, have in common that is different from being grouped in another one. A correlation between the three involved parameters can be found taking into account that the y-axes (one represented by impedance, the other one represented by resonance frequency) are comparable to each other because the lower point represents larger muscle mass or lower fat content. With that said, looking at the leg section in both Figures 4.11 and 4.12, for example subjects 9 remains at the same position in the space, while subject 10 shifts downwards with respect to the resonance frequency. This is interesting because this would show that participant 10 has higher muscle contents compare to participant 9. This does not happen in all the groups; therefore, this aspect needs to be better studied considering these specific details.

Another example can be done from Figure 4.12 considering subject 7 in the upper arm graph. Participant 7 shows the highest peak of resonance frequency among the subjects and this would be due to the young age (16 years) and thus the muscular structure is not well defined as well as all the other subjects.

Furthermore, what it can be seen from both Figures 4.11 and 4.12 is that, most of the cases, the higher the compressibility, the more the frequency peaks shift to the lower point. This behaviour cannot be seen for example in the case of the upper arm in Figure 4.11 where a homogeneous distribution is obtained.

However, it is needed to better analyse these data and to come up with hypotheses that have to be validated. Some of the hypotheses could be:

1. The lower the compressibility, the higher the impedance;

2. The lower the compressibility, the higher the resonance frequency.

These hypotheses could only be validated with further measurements (see Chapter5) that will give an idea of why some participants are grouped in specific groups and other subjects belong to other groups. These considerations will help to better characterize biological tissues getting more information that derive not only from the anthropometric characteristics but also from different methods such as compressibility test, resonance parameters and bioimpedance data.

Chapter 5

Conclusions and Future work

In this thesis, significant measurements were collected at high and low frequencies to achieve an overall characterization of specific body segments. This research study is part of the H2020 European SINTEC Project in which one of the main goals is the design of an implantable antenna that will allow the communication from many sensor nodes on the body.

However, the antenna design is still an aspect that has to be better investigated. As the human body can act as a conductive system, an important parameter that has to be optimized as much as possible is the biocompatibility for the realization of a suitable antenna. In fact, it has to be well connected to the body and therefore, this work is carried out not only to optimize sensors and antenna design, but also to obtain additional information for improving the measurement accuracy and the portability of the final application.

Nevertheless, there are still some aspects that need to be investigated, reported below:

1. **Increase the size of the dataset**: since the available dataset is not large, it is important to collect much more data for better evaluating the algorithm performance. Furthermore, it is also fundamental to have a wider dataset which include the elderly, children and young subjects.

2. **Improve the repeatability of bioimpedance measurements**: unlike the collected SRR data, the bioimpedance measurements have been acquired only once for each body segment because of the limited availability of the measuring instrument. Therefore, bioimpedance signals have to be collected at least twice.

3. **Additional ultrasound measurements**: this methodology would be very interesting for evaluating the thickness of specific tissues such as skin, fat, and muscle. This can be supportive for the body tissue characterization.

4. **Combination of low and high frequency approaches**: an interesting idea is that the high and low frequencies measurements can be performed simultaneously by using only one device that includes both SRR and disposable patch.

5. **Extraction of empirical models**: since in the present study important correlations among the results are found, empirical models should be defined starting from hypotheses that have to be validated.

6. **Evaluation of the intra-body communication**: Another open issue of the SINTEC project is to use adipose tissue as a communication channel to transmit information among different sensors placed on the body. To ensure this, the current idea is to use implanted repeater antennas every 10 centimeters. This distance has been chosen as it is the upper limit beyond which the signal would be dispersed [71]. From the results obtained in this work, it can be seen that the upper arm is a good position where the final sensor can be applied to since it is the body segment that shows the highest impedance and therefore highest fat content. Moreover, this is also a comfortable area unlike hands, feet, and head which were not considered because they have different anatomy and lower fat content. Obviously, this has to be proved using more data.

7. **Phantom development**: the ultimate goal is to perform the present experiment not only considering the human body but also on phantom-based demonstrators that are able to mimic humans as much as possible. This is one of the objectives of the SINTEC Project as well.

Appendix A: Informed consent form

INFORMED CONSENT RELEASE

Investigator:

My name is Rocco Calzone, I am a biomedical engineering student at Politecnico di Torino (Italy) and I am working on my master's thesis at Uppsala University (Sweden).
I am inviting you to participate in a research study. Involvement in the study is voluntary, so you may choose to participate or not. I am now going to explain the study to you. Please feel free to ask any questions that you may have about the research; I will be happy to explain anything in greater detail.

I am interested in learning more about the conductance phenomenon, the impedance parameters and other physical properties in biological materials in order to characterize the human body composition. You will be asked to sit in a chair maintaining your muscles in a relax state and data collection will be performed. This will take approximately 20 minutes of your time. All information will be kept secure in the database of the Microwave in Medical Engineering Group (MMG), Solid State Electronics Division, Engineering Sciences Department, Uppsala University. If anonymous, this means that your name will not appear anywhere and no one except me will know about your specific answers. If confidential, I will assign a number to your responses, and only I will have the key to indicate which number belongs to which participant. In any articles I write or any presentations that I make, I will use a made-up name for you, and I will not reveal details or I will change details about where you work, where you live, any personal information about you, and so forth.

The benefit of this research is that you will be helping me to collect data from different body segments and they will be conserved in my thesis report. This information should help me to better understanding how to optimize sensors and antenna design in the context of the SINTEC Project (www.sintec-project.eu). There are no risks for participating in this study due to the non-invasiveness of the technique, which consists of injecting an electric current into your body for measuring the bioimpedance from different parts of your body.

Participant:

All of my questions and concerns about this study have been addressed. I choose, voluntarily, to participate in this research project. I certify that I am at least 18 years of age or I am responsible (parent) of the subject concerned.

[redacted]
print name of participant

[redacted] 5th July 2019
signature of participant date

Rocco Calzone
print name of investigator

Rocco Calzone 5th July 2019
signature of investigator date

(informed consent) p. 1 of 1

Appendix B: LabVIEW Code Block

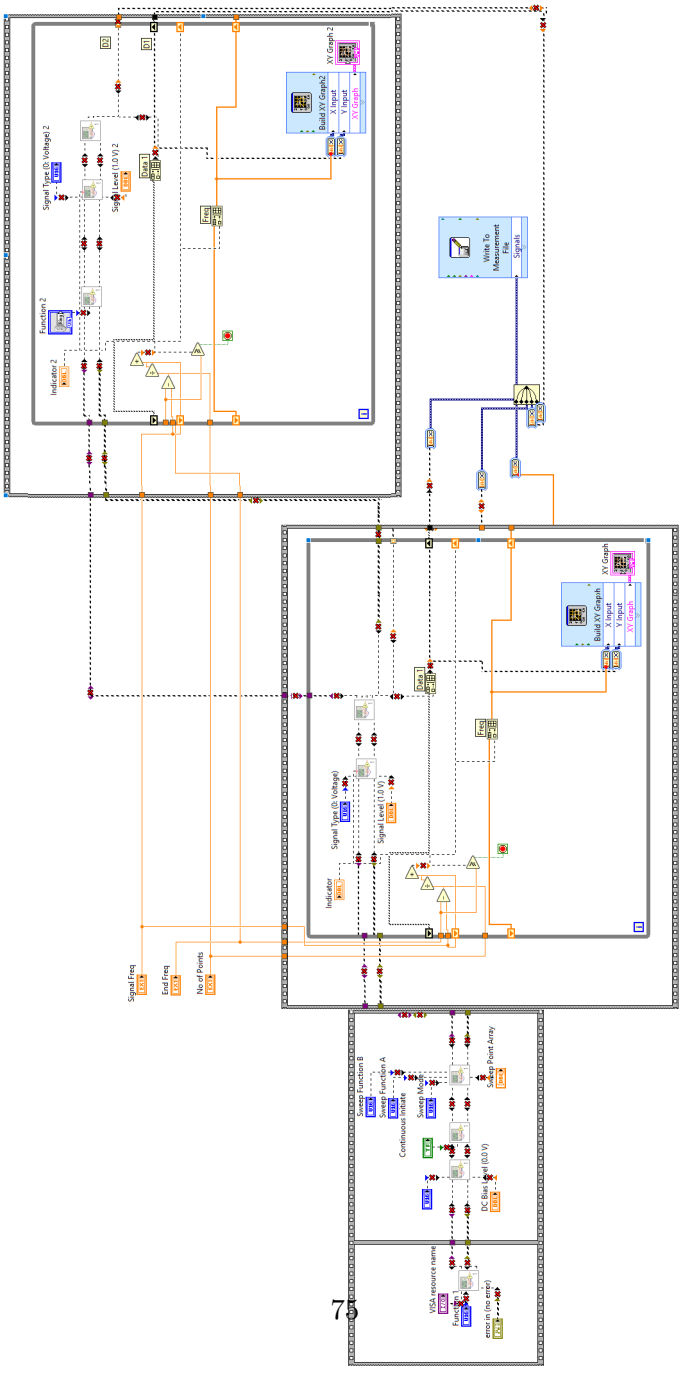

Bibliography

[1] J. Pan and W. J. Tompkins, "A real-time qrs detection algorithm," *IEEE Trans. Biomed. Eng*, vol. 32, no. 3, pp. 230–236, 1985.

[2] Sintec website. [Online]. Available: http://www.sintec-project.eu/

[3] Image from the sintec project video. [Online]. Available: https://www.youtube.com/watch?v=PkdL_Va9kRA&amp=;t=10s

[4] K. Hachisuka, A. Nakata, T. Takeda, K. Shiba, K. Sasaki, H. Hosaka, and K. Itao, "Development of wearable intra-body communication devices," *Sensors and actuators A: physical*, vol. 105, no. 1, pp. 109–115, 2003.

[5] Bio-impedance analysis definition. [Online]. Available: http://florey.biosci.uq.edu.au/BIA/

[6] R. Calzone, G. Pagana, M. D. Perez, and R. Augustine, "Innovations in biomedicine: Measuring physiological parameters becomes as simple as applying a plaster on the body," in *2019 International Conference on Electromagnetics in Advanced Applications (ICEAA)*. IEEE, 2019, pp. 1443–1446.

[7] D. Bann, D. Kuh, A. K. Wills, J. Adams, S. Brage, R. Cooper, N. S. of Health, D. Scientific, and D. C. Team, "Physical activity across adulthood in relation to fat and lean body mass in early old age: findings from the medical research council national survey of health and development, 1946–2010," *American journal of epidemiology*, vol. 179, no. 10, pp. 1197–1207, 2014.

[8] C. Meisinger, A. Döring, B. Thorand, M. Heier, and H. Löwel, "Body fat distribution and risk of type 2 diabetes in the general population: are there differences between men and women? the monica/kora augsburg cohort study," *The American journal of clinical nutrition*, vol. 84, no. 3, pp. 483–489, 2006.

[9] P. A. Codner, K. Shields, M. Kappus, B. Collier, M. Rosenthal, and R. G. Martindale, "Comparative measures of lean body tissues in the clinical setting," *Current Nutrition Reports*, vol. 5, no. 3, pp. 191–198, 2016.

[10] Y. Yamada, K. Matsuda, M. P. Björkman, and M. Kimura, "Application of segmental bioelectrical impedance spectroscopy to the assessment of skeletal muscle cell mass in elderly men," *Geriatrics & gerontology international*, vol. 14, pp. 129–134, 2014.

[11] G. Greenhall and A. Davenport, "Screening for muscle loss in patients established on peritoneal dialysis using bioimpedance," *European journal of clinical nutrition*, vol. 71, no. 1, p. 70, 2017.

[12] S. Smith and A. Madden, "Body composition and functional assessment of nutritional status in adults: a narrative review of imaging, impedance, strength and functional techniques," *Journal of human nutrition and dietetics*, vol. 29, no. 6, pp. 714–732, 2016.

[13] [Online]. Available: https://www.nsca.com/education/articles/kinetic-select/sport-performance-and-body-composition/

[14] S. F. Khalil, M. S. Mohktar, and F. Ibrahim, "The theory and fundamentals of bioimpedance analysis in clinical status monitoring and diagnosis of diseases," *Sensors*, vol. 14, no. 6, pp. 10 895–10 928, 2014.

[15] D. J. Gibson, S. T. Burden, B. J. Strauss, C. Todd, and S. Lal, "The role of computed tomography in evaluating body composition and the influence of reduced muscle mass on clinical outcome in abdominal malignancy: a systematic review," *European journal of clinical nutrition*, vol. 69, no. 10, p. 1079, 2015.

[16] D. Bracco, D. Thiébaud, R. L. Chioléro, M. Landry, P. Burckhardt, and Y. Schutz, "Segmental body composition assessed by bioelectrical impedance analysis and dexa in humans," *Journal of Applied Physiology*, vol. 81, no. 6, pp. 2580–2587, 1996.

[17] N. Abate, A. Garg, R. Coleman, S. M. Grundy, and R. M. Peshock, "Prediction of total subcutaneous abdominal, intraperitoneal, and retroperitoneal adipose tissue masses in men by a single axial magnetic resonance imaging slice," *The American journal of clinical nutrition*, vol. 65, no. 2, pp. 403–408, 1997.

[18] T. Erselcan, F. Candan, S. Saruhan, and T. Ayca, "Comparison of body composition analysis methods in clinical routine," *Annals of nutrition and metabolism*, vol. 44, no. 5-6, pp. 243–248, 2000.

[19] C. H. Ling, A. J. de Craen, P. E. Slagboom, D. A. Gunn, M. P. Stokkel, R. G. Westendorp, and A. B. Maier, "Accuracy of direct segmental multi-frequency bioimpedance analysis in the assessment of total body and segmental body composition in middle-aged adult population," *Clinical nutrition*, vol. 30, no. 5, pp. 610–615, 2011.

[20] M. Y. Jaffrin and H. Morel, "Body fluid volumes measurements by impedance: A review of bioimpedance spectroscopy (bis) and bioimpedance analysis (bia) methods," *Medical engineering & physics*, vol. 30, no. 10, pp. 1257–1269, 2008.

[21] U. G. Kyle, I. Bosaeus, A. D. De Lorenzo, P. Deurenberg, M. Elia, J. M. Gómez, B. L. Heitmann, L. Kent-Smith, J.-C. Melchior, M. Pirlich *et al.*, "Bioelectrical impedance analysisâpart i: review of principles and methods," *Clinical nutrition*, vol. 23, no. 5, pp. 1226–1243, 2004.

[22] L. Ward, N. Byrne, K. Rutter, L. Hennoste, A. Hills, B. Cornish, and B. Thomas, "Reliability of multiple frequency bioelectrical impedance analysis: an intermachine comparison," *American Journal of Human Biology: The Official Journal of the Human Biology Association*, vol. 9, no. 1, pp. 63–72, 1997.

[23] R. Pethig, "Dielectric properties of body tissues." *Clinical physics and physiological measurement: an official journal of the Hospital Physicists' Association, Deutsche Gesellschaft fur Medizinische Physik and the European Federation of Organisations for Medical Physics*, vol. 8, pp. 5–12, 1987.

[24] J. E Hall, *Guyton and Hall textbook of medical physiology.* Elsevier Inc., 2016.

[25] [Online]. Available: https://www.ncbi.nlm.nih.gov/pmc/articles/PMC2597841/pdf/nihms43147.pdf

[26] S. Berlit, J. Brade, B. Tuschy, E. Foeldi, U. Walz-Eschenlohr, H. Leweling, and M. Suetterlin, "Whole-body versus segmental bioelectrical impedance analysis in patients with edema of the upper limb after breast cancer treatment," *Anticancer research*, vol. 33, no. 8, pp. 3403–3406, 2013.

[27] [Online]. Available: https://tspace.library.utoronto.ca/bitstream/1807/92574/1/Gavrilovic_Bojan_201611_MHSc_thesis.pdf

[28] H. P. Schwan, "Electrical properties of tissue and cell suspensions," in *Advances in biological and medical physics.* Elsevier, 1957, vol. 5, pp. 147–209.

[29] [Online]. Available: https://www.mn.uio.no/fysikk/english/research/projects/bioimpedance/whatis/

[30] American council on exercise. [Online]. Available: https://www.acefitness.org/education-and-resources/lifestyle/tools-calculators/percent-body-fat-calculator

[31] D. Schoeller and R. Kushner, "Determination of body fluids by the impedance technique," *IEEE Engineering in Medicine and Biology Magazine*, vol. 8, no. 1, pp. 19–21, 1989.

[32] A. Tagliabue, A. Andreoli, M. Comelli, S. Bertoli, G. Testolin, G. Oriani, and A. De Lorenzo, "Prediction of lean body mass from multifrequency segmental impedance: influence of adiposity," *Acta diabetologica*, vol. 38, no. 2, pp. 93–97, 2001.

[33] [Online]. Available: https://iopscience.iop.org/article/10.1088/0967-3334/29/5/009/pdf

[34] U. G. Kyle, L. Genton, L. Karsegard, D. O. Slosman, and C. Pichard, "Single prediction equation for bioelectrical impedance analysis in adults aged 20–94 years," *Nutrition*, vol. 17, no. 3, pp. 248–253, 2001.

[35] H. C. Lukaski, W. W. Bolonchuk, C. B. Hall, and W. A. Siders, "Validation of tetrapolar bioelectrical impedance method to assess human body composition," *Journal of applied physiology*, vol. 60, no. 4, pp. 1327–1332, 1986.

[36] M. Thomasset, "Bioelectric properties of tissue. impedance measurement in clinical medicine. significance of curves obtained," *Lyon medical*, vol. 94, p. 107, 1962.

[37] J. Simpson, D. Lobo, J. Anderson, I. Macdonald, A. Perkins, K. Neal, S. Allison, and B. Rowlands, "Body water compartment measurements: a comparison of bioelectrical impedance analysis with tritium and sodium bromide dilution techniques," *Clinical Nutrition*, vol. 20, no. 4, pp. 339–343, 2001.

[38] M. G. O. Rikkert, P. Deurenberg, R. W. Jansen, M. A. van't Hof, and W. H. Hoefnagels, "Validation of multi-frequency bioelectrical impedance analysis in detecting changes in fluid balance of geriatric patients," *Journal of the American Geriatrics Society*, vol. 45, no. 11, pp. 1345–1351, 1997.

[39] A. De Lorenzo, A. Andreoli, J. Matthie, and P. Withers, "Predicting body cell mass with bioimpedance by using theoretical methods: a technological review," *Journal of applied physiology*, vol. 82, no. 5, pp. 1542–1558, 1997.

[40] E. Pittella, E. Piuzzi, E. Rizzuto, S. Pisa, and Z. Del Prete, "Metrological characterization of a combined bio-impedance plethysmograph and spectrometer," *Measurement*, vol. 120, pp. 221–229, 2018.

[41] F. Zhu, M. Kuhlmann, G. Kaysen, S. Sarkar, C. Kaitwatcharachai, R. Khilnani, L. Stevens, E. Leonard, J. Wang, S. Heymsfield *et al.*, "Segment-specific resistivity improves body fluid volume estimates from bioimpedance spectroscopy in hemodialysis patients," *Journal of Applied Physiology*, vol. 100, no. 2, pp. 717–724, 2006.

[42] J. Moon, "Body composition in athletes and sports nutrition: an examination of the bioimpedance analysis technique," *European journal of clinical nutrition*, vol. 67, no. S1, p. S54, 2013.

[43] F. Seoane, S. Abtahi, F. Abtahi, L. Ellegård, G. Johannsson, I. Bosaeus, and L. C. Ward, "Mean expected error in prediction of total body water: a true accuracy comparison between bioimpedance spectroscopy and single frequency regression equations," *BioMed research international*, vol. 2015, 2015.

[44] T. H. Cole, "Development of a novel device for non-invasive leg fluid volume measurements," Ph.D. dissertation, 2018.

[45] S. Raman, R. Augustine, and A. Rydberg, "Noninvasive osseointegration analysis of skull implants with proximity coupled split ring resonator antenna," *IEEE Transactions on Antennas and Propagation*, vol. 62, no. 11, pp. 5431–5436, 2014.

[46] Beneli website. [Online]. Available: https://beneli.se/

[47] Keysight e4980a precision lcr meter datasheet. [Online]. Available: https://literature.cdn.keysight.com/litweb/pdf/5989-4435EN.pdf

[48] T. Dowrick, C. Blochet, and D. Holder, "In vivo bioimpedance measurement of healthy and ischaemic rat brain: implications for stroke imaging using electrical impedance tomography," *Physiological measurement*, vol. 36, no. 6, p. 1273, 2015.

[49] T. Freeborn and B. Fu, "Fatigue-induced cole electrical impedance model changes of biceps tissue bioimpedance," *Fractal and Fractional*, vol. 2, no. 4, p. 27, 2018.

[50] D. N. Huu, D. Kikuchi, O. Maruyama, A. Sapkota, and M. Takei, "Cole-cole analysis of thrombus formation in an extracorporeal blood flow circulation using electrical measurement," *Flow Measurement and Instrumentation*, vol. 53, pp. 172–179, 2017.

[51] R. Gudivaka, D. Schoeller, R. Kushner, and M. Bolt, "Single-and multifrequency models for bioelectrical impedance analysis of body water compartments," *Journal of Applied Physiology*, vol. 87, no. 3, pp. 1087–1096, 1999.

[52] D. Ayllon, F. Seoane, and R. Gil-Pita, "Cole equation and parameter estimation from electrical bioimpedance spectroscopy measurements-a comparative study," in *2009 Annual International Conference of the IEEE Engineering in Medicine and Biology Society*. IEEE, 2009, pp. 3779–3782.

[53] G. P. Pichler, O. Amouzadeh-Ghadikolai, A. Leis, and F. Skrabal, "A critical analysis of whole body bioimpedance spectroscopy (bis) for the estimation of body compartments in health and disease," *Medical engineering & physics*, vol. 35, no. 5, pp. 616–625, 2013.

[54] S. Redzwan Mohd Shah, "Prospective applications of microwaves in medicine: Microwave sensors for orthopedic monitoring and burn depth assessment," Ph.D. dissertation, Acta Universitatis Upsaliensis, 2019.

[55] V. Mattsson, "Clinical data analysis for conceptual proof of microwave bone healing monitoring system for craniosynostosis patients," 2018.

[56] J. Velander, "Microwave sensor measurements and human tissue characterization," 2016.

[57] Resonator. [Online]. Available: https://en.wikipedia.org/wiki/Resonator

[58] Ism band. [Online]. Available: https://en.wikipedia.org/wiki/ISM_band

[59] Mini vna. [Online]. Available: http://miniradiosolutions.com/54-2/

[60] D. Andreuccetti, R. Fossi, and C. Petrucci, "Dielectric properties of body tissues in the frequency range 10 hz–100 ghz," *Nello Carrara" Institute of Applied Physics*, vol. 1, 1997.

[61] K. Karastergiou, S. R. Smith, A. S. Greenberg, and S. K. Fried, "Sex differences in human adipose tissues–the biology of pear shape," *Biology of sex differences*, vol. 3, no. 1, p. 13, 2012.

[62] S. Mohd Shah, J. Velander, P. Mathur, M. Perez, N. Asan, D. Kurup, T. Blokhuis, and R. Augustine, "Split-ring resonator sensor penetration depth assessment using in vivo microwave reflectivity and ultrasound measurements for lower extremity trauma rehabilitation," *Sensors*, vol. 18, no. 2, p. 636, 2018.

[63] Compressibility. [Online]. Available: https://en.wikipedia.org/wiki/Compressibility

[64] C. Tanner, J. A. Schnabel, D. L. Hill, D. J. Hawkes, M. O. Leach, and D. R. Hose, "Factors influencing the accuracy of biomechanical breast models," *Medical physics*, vol. 33, no. 6Part1, pp. 1758–1769, 2006.

[65] A. Natali, C. Fontanella, and E. Carniel, "A numerical model for investigating the mechanics of calcaneal fat pad region," *Journal of the Mechanical Behavior of Biomedical Materials*, vol. 5, no. 1, pp. 216–223, 2012.

[66] S. Grimnes and Ø. Martinsen, "Bioimpedance wiley encyclopedia of biomedical engineering," 2006.

[67] M. Fenech and M. Y. Jaffrin, "Extracellular and intracellular volume variations during postural change measured by segmental and wrist-ankle bioimpedance spectroscopy," *IEEE transactions on biomedical engineering*, vol. 51, no. 1, pp. 166–175, 2004.

[68] Weight of human body parts. [Online]. Available: http://robslink.com/SAS/democd79/body_part_weights.htm

[69] F. Zhu, M. Carter, S. Thijssen, P. Kotanko, and N. W. Levin, "Estimation of body composition in dialysis patients using segmental bioimpedance," in *2009 3rd International Conference on Bioinformatics and Biomedical Engineering*. IEEE, 2009, pp. 1–4.

[70] K. J. Shafer, W. A. Siders, L. K. Johnson, and H. C. Lukaski, "Validity of segmental multiple-frequency bioelectrical impedance analysis to estimate body composition of adults across a range of body mass indexes," *Nutrition*, vol. 25, no. 1, pp. 25–32, 2009.

[71] N. B. Asan, "Fat-ibc: A new paradigm for intra-body communication," Ph.D. dissertation, Acta Universitatis Upsaliensis, 2019.